ISSN(Online) : 2319-8753
ISSN (Print) : 2347-6710

International Journal of Innovative Research in Science, Engineering and Technology

(An ISO 3297: 2007 Certified Organization)

Website: www.ijirset.com

Vol. 6, Issue 2, February 2017

Influence of Waste Cooking Oil Temperature on Wear and Frictional Behaviour of Metals Sliding against Stainless Steel Counterface

J.G. Alotaibi, Ayedh Alajmi

Department of Automotive and Marine Engineering Technology, Public Authority for Applied Education and Training, Kuwait

ABSTRACT: The development of recycled, renewable and sustainable products to replace fossil products is a vital concern from industrial, environmental and academic viewpoints. Lubricants are one of the synthetic products widely used in numerous fields of the manufacturing and industrial sectors. Furthermore in 2005, more than 38 million metric tons of oils were used in the lubrication techniques of various industrial applications in the United States (US). In other words, the need for alternative friendly lubricants needs to increase by about 36 billion gallons to meet expected demands in 2022. This need motivates the current investigation of the potential use of waste cooking oil as a lubricant for tribological applications. A review of the available literature reviewed no work related to this topic. However, many works have been conducted on vegetable oils and their potential as lubricant. The current study establishes the basis for the research in the area of waste cooking oil as a lubricant; focusing on the oil and its blend characteristics and applications in journal bearings.

At the first stage of this study, comprehensive experiments were conducted on the wear and the frictional behaviour of brass, aluminium and mild steel metals sliding against a stainless steel counterface under dry contact condition for comparison purposes with the lubricant results. Furthermore, predicting the tribological performance of materials is a very complex task and many attempts to model the wear and frictional behaviour of materials have failed. In this study, the artificial neural networks approach is used as a tool to predict wear, roughness, interface temperature and the frictional behaviour of metals under different operating parameters.

For the wear experiments under dry contact conditions, the wear and frictional performance of brass, aluminium and mild steel metals was investigated at different operating parameters: sliding distances (0 – 10.8 km) and applied loads (0 – 50 N) against a stainless steel counterface at a sliding velocity of 2.8 m/s. Experiments were performed using a block-on-ring (BOR) machine. To categorise the wear mechanism and damage features on the worn surfaces and the collected debris, scanning electron microscopy was used. A thermal imager was used to measure the interface temperature between the contacted bodies.

The results of the dry tests revealed that the operating parameters significantly influence the wear and frictional behaviour of all the metals. Brass metal exhibited better wear and frictional behaviour compared to the other metals tested. This is mainly due to the presence of 4% of Pb which helped reduce the aggressiveness of the material removal. Three different wear mechanisms were observed: two-body abrasion (brass), three-body abrasion (mild steel) and adhesive (aluminium). Friction coefficient trends were almost steady for brass and mild steel, however, aluminium/stainless steel exhibited slight fluctuations due to the modifications of the worn surface due to the sliding.

A biolubricant extracted from waste cooking oil (WCO) was developed in this study. Different blends of lubricant were prepared: fully synthetic 100%SO, 75%SO+25%WCO, 50%SO+50%WCO 25%SO+75%WCO and 100%WCO. The prepared waste cooking oil was blended with 5% (wt) of EVA copolymer and 2% (wt) of EC and synthetic oils. Viscosity, pour point and flash points of the blends were examined and compared with industrial lubricants, (10W-50, 15W-40, 5W-40, and 5W-30).

ISSN(Online) : 2319-8753
ISSN (Print) : 2347-6710

International Journal of Innovative Research in Science, Engineering and Technology

(An ISO 3297: 2007 Certified Organization)

Website: www.ijirset.com

Vol. 6, Issue 2, February 2017

The possibility of using WCO with its blend as a lubricant was tested using two techniques. First, a new tribology machine was designed and fabricated locally to study the wear and frictional performance of brass, aluminium and mild steel under lubricant conditions considering different sliding distances (up to 10.8 km), applied loads (10 N – 40 N) and sliding speed of 2.8 m/s at different lubricant temperatures (22^{o}C, 40^{o}C, 80^{o}C). For consistent comparison purposes with the dry data, 113 kPa applied pressure was used as the dry contact condition was conducted mainly on 50N applied load which is equivalent to 113 kPa.
This study found promising potential for the use of WCO as a lubricant from a viscosity viewpoint. The viscosity of the waste cooking oil was significantly enhanced with the addition of 5% (wt) of EVA copolymer and 2% (wt) of EC. Blending the waste cooking oil with the fully synthetic oil also showed good improvement in performance. Based on the viscosity data, it is found that the pure waste cooking oil is very comparable with W5-30 oil which is recommended for gasoline and diesel engines. Increasing the applied load reduced the specific wear rate due to the presence of the lubricant which assisted to absorb the heat in the interface and clear (polish) the rubbed surfaces. The lubricant temperature was the key in determining the wear behaviour of the materials. Increasing the temperature reduced the viscosity, leading to less lifting during the experiments (i.e. a high specific wear rate). Conversely, the lubricant temperature showed no remarkable influence on the frictional behaviour. This is mainly due to the chemical adsorption of the fatty acids on the worn surfaces which acted as coated layer. From the journal bearing testing results, the waste cooking oil and its blends exhibited a similar trend in oil pressure values to the ones obtained for the fully synthetic oil, thus demonstrating the potential of waste cooking oil and its blends for journal bearing applications.

The complexity of predicting the wear and frictional performance of the materials motivates the tribologist to adopt an artificial neural network (ANN) approach, as it can be used to make such predictions with caution. In developing an ANN for this study, training function, performance and adopting functions were found to be the keys to predicting wear, roughness and interface temperature. The large input data of the friction coefficient (12009 x 3 x 3) made the prediction of friction coefficient difficult and led to poor ANN performance. Using individual inputs for each parameter and training the ANN in several steps improved the performance. About 95.5% prediction performance was recorded, particularly for the wear, roughness and interface temperature.

I. INTRODUCTION

Materials preparation and experimental procedure

This chapter discusses the preparation and extraction of WCO and its blending procedure with SO. The metal selections and their fundamental characteristics, the experimental setup and procedure for the dry adhesive wear testings, and the new concept of the new tribology machine associated with this experimental procedure are also introduced.

II. PREPARATION OF MATERIALS

A. WASTE COOKING OIL PREPARATIONS

WCO can be obtained from different sources such as restaurants and fast-food outlets. For this study, WCO was collected from fish and chips restaurants in Toowoomba city, Queensland, Australia. Based on information obtained from the restaurant owners, fish and chips are cooked in cotton seeds oil at a temperature of 180 ^{o}C. The oil is used for seven days and it heated up for seven hours a day (from 10 am to 5 pm), i.e. the oil is used for 49 hours. For one restaurant, about 10 litres of oil need to be disposed of daily. The collected oil was placed in a 200-litre tank. The steps involved in cleaning and preparing the oil are described in Figure 3.1. The collected oil was dirty and full of undesirous substances (e.g. small burnt chips or leftover fish). In order to purify it, different-sized sieves were used to extract the debris. The oil was then heated to 90–100^{o}C in order to remove the moisture from it. The oil was kept at this temperature for about one hour. While the oil was cooling down, it was filtered using a micro-filter (woven mesh fabrics) supplied by Sefar Filter, Australia. This type of filter is recommended for filtering chemicals as it is able to resist high temperatures. The fabrics used in designing the filter have thread diameters < 250 µm and mesh openings <

ISSN(Online) : 2319-8753
ISSN (Print) : 2347-6710

International Journal of Innovative Research in Science, Engineering and Technology

(An ISO 3297: 2007 Certified Organization)

Website: www.ijirset.com

Vol. 6, Issue 2, February 2017

500 µm and can be ultrasonically welded. The main characteristics of the fabric used in the filter are high dimensional stability and tensile strength, constant fabric stiffness and thickness, repeatable pore size and filtration performance, low pressure drop and high flow rate.

Before blending the waste cooking oil with the synthetic oil, 5% (wt) of EVA copolymer and 2% (wt) of EC were used as additives. Their impact will be discussed later in this chapter. Different blend ratios were used in preparing the blends of the waste cooking oil (WCO) and fully synthetic oil (SO) as lubricants: 0, 25 vol. %, 50 vol. %, 75 vol. % and 100 vol. % of WCO in SO. 5w-30 fully synthetic oil is used in this work which was supplied by Shell Helix. The technical data for each oil grade is provided by the company via http://www.shell.com/global/products-services/on-the-road/oils-lubricants. Some of the fully synthetic oil specification are MRV, ASTM D4684 (17000), Density, ASTM D4052 (852), Flash point, ASTM D92 (240), Pour point, ASTM D97 (-48).

The WCO was heated up to 80^{o}C and the SO was gently added in about 5% increments to reach the required percentage. An electrical mixer was used to mix the blends at 80^{o}C for about 30 mins. The blends were cooled down to room temperature and kept in glass containers to prevent any chemical reaction or moisture absorption. In the last stage of this work, different blends were used for journal bearing tests.

The fatty acids composition of the pure WCO has been tested with the GC-FID technique under the operating condition of an oven: 150 ^{o}C (75.0 min) isothermal, Carrier: helium, 21 cm/sec at 150 ^{o}C, and Detector: FID, 250 ^{o}C. The results of the fatty acids composites of the WCO are presented in Table 3.1.

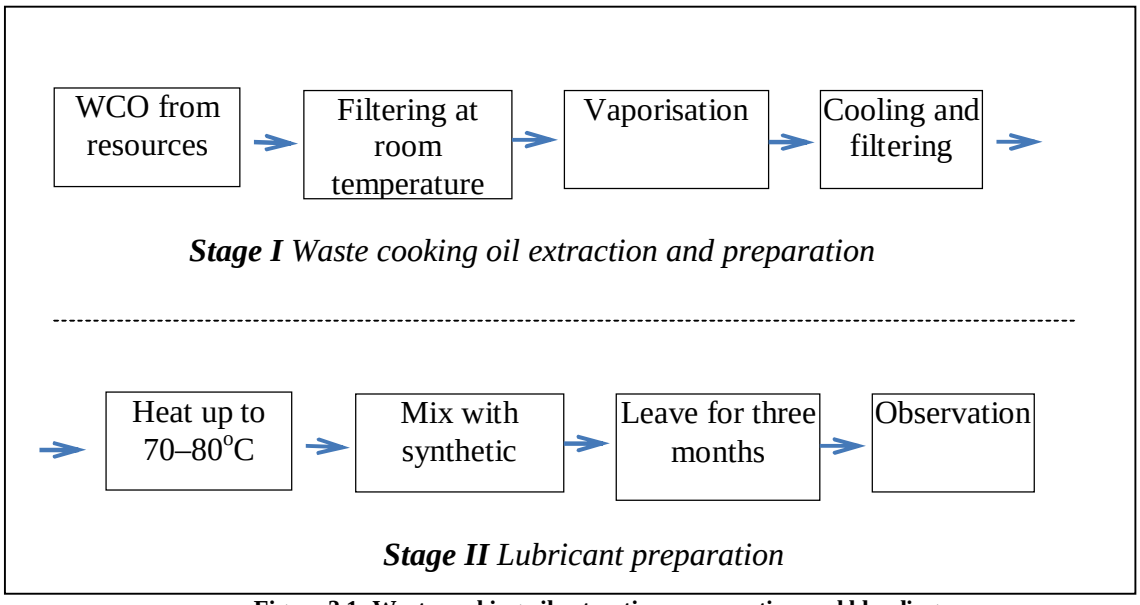

Figure 3.1: Waste cooking oil extraction, preparation and blending

ISSN(Online) : 2319-8753
ISSN (Print) : 2347-6710

International Journal of Innovative Research in Science, Engineering and Technology

(An ISO 3297: 2007 Certified Organization)

Website: www.ijirset.com

Vol. 6, Issue 2, February 2017

Table 3.1: Fatty Acid Composition of the Collected Waste Cooking Oil

Fatty Acid Composition	%
Myristic (14:0)	0.9
Palmitic (16:0)	21.9
Palmitoleic (16:1)	0.1
Stearic (18:0)	5.2
Oleic (18:1)	41.0
Linoleic (18:2)	29.3
Linolenic (18:3)	0.7
Additives (unknown)	0.9

There is little research on the influence of the chemical compositions of WCO on the tribological behaviour of metals. However, Majdoub, Martin [1] recently reported that oleic and linoleic have been used as additives for PAO4 oil to reduce the friction coefficient. Their results showed that the addition of about 1% of those fatty acids assisted in reducing the energy loss due to the adhesive rubbing process, reducing the friction coefficient. Ikeda, Tomohiro [2] investigated the influence of palmitic, stearic, oleic and linoleic acids on palm oil as a lubricant and found that stearic gained optimum results in terms of the wear and frictional performance of the palm oil.

B. METALS SELECTION

In the literature there are several materials are selected for tribological applications in such things as bearings and bushes. Among the most common and recent materials used under dry and lubricant contact conditions are mild steel [3, 4], brass [5, 6] and aluminium [7, 8]. Mild steel (SAE 1020, chemical composition: C=0.20%, Mn=0.45%, P=0.04% max, S=0.05% max), aluminium (6060) and commercial brass (58 Cu, 4% Pb and 38% Zn) have been selected for the current study. Samples were prepared from 50 mm x 20 mm x 25 mm blocks of the material using the milling machine at the University of Southern Queensland. Some of the supplied properties of the materials are given in Table 3.2. For the counterface materials, the experiments were conducted against a stainless steel ring (AISI 304).

Table 3.2: Properties of Mild Steel, Aluminium and Brass

Materials	$б_y$ MPa	$б_u$ MPa	E GPa	Elongation, %	Hardness HB
Mild steel	380	480	200	15	73
Aluminium alloy	180	220	69.5	13	45
Brass	310	430	96	27	62
Stainless steel (AISI 304)	621	290	28	55	82

III. HYBRID TRIBOLOGICAL MACHINE

As was mentioned in Chapter 2, most the experiments in the literature were conducted to study the viscosity of the oil at different temperature and/or the tribological performance of metal contacts under lubricant conditions at room temperature. Because oil may be used at elevated temperatures, the combination of interface and environmental temperatures may affect the interaction behaviour of the asperities in contact, and so affect the real application of the oil. This factor is considered in the design of the project's new machine.

A. THE BLOCK-ON-RING CONCEPT

Tribological testing can be done by various laboratory tribo-machines such as pin-on-disc (POD), ASTM G99, block-on-ring (BOR), ASTM G77 or G137-953, dry sand rubber wheel (DSRW), ASTM G655, wet sand rubber wheel

ISSN(Online) : 2319-8753
ISSN (Print) : 2347-6710

International Journal of Innovative Research in Science, Engineering and Technology

(An ISO 3297: 2007 Certified Organization)

Website: www.ijirset.com

Vol. 6, Issue 2, February 2017

(WSRW), ASTM G105, as well as the sand/steel wheel test under wet/dry conditions (ASTM B611; [9]. For the current study, a BOR configuration was selected due to its popularity amongst researchers in the field of lubricants. In this configuration (Figure 3.2), a block of the material was pressed using a dead weight onto a rotating ring (counterface). The rubbing process began with line/line contact and increased to area/area contact, thereby varying the contact area at the running-in stage. This assisted in understanding the integration of the asperities in contact at the initial stages of the sliding process.

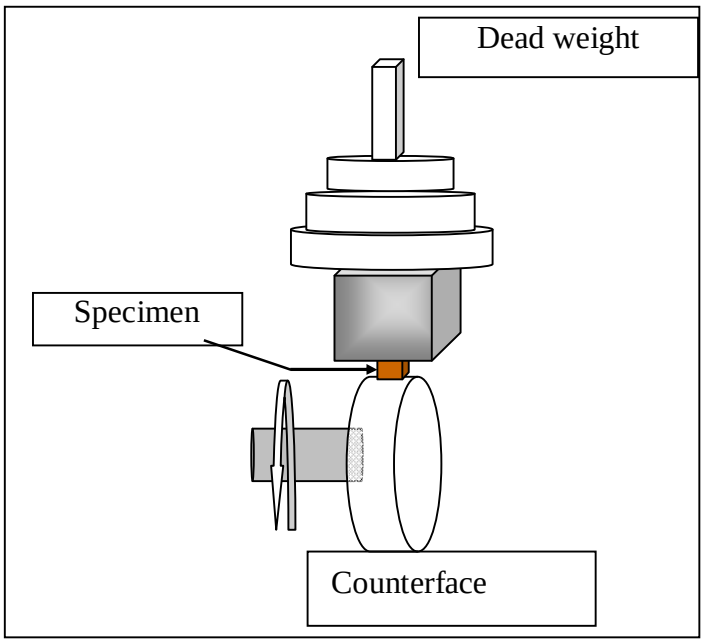

Figure 3.2: Block-on-ring technique

II. INTEGRATION OF LUBRICANT TEMPERATURE IN THE NEW MACHINE

The addition of the lubricant container can be implemented in the technique associated with the lubricant heater to heat up the lubricant temperature during the test. CATIA software was used to design the new components for the machine. Figure 3.3 presents a three-dimensional drawing of the newly designed machine and lists its main components. The main purpose of the machine is to provide tribological environments under lubricant condition. A detailed drawing of all the main parts of the machine is provided in appendix A.

ISSN(Online) : 2319-8753
ISSN (Print) : 2347-6710

International Journal of Innovative Research in Science, Engineering and Technology

(An ISO 3297: 2007 Certified Organization)

Website: www.ijirset.com

Vol. 6, Issue 2, February 2017

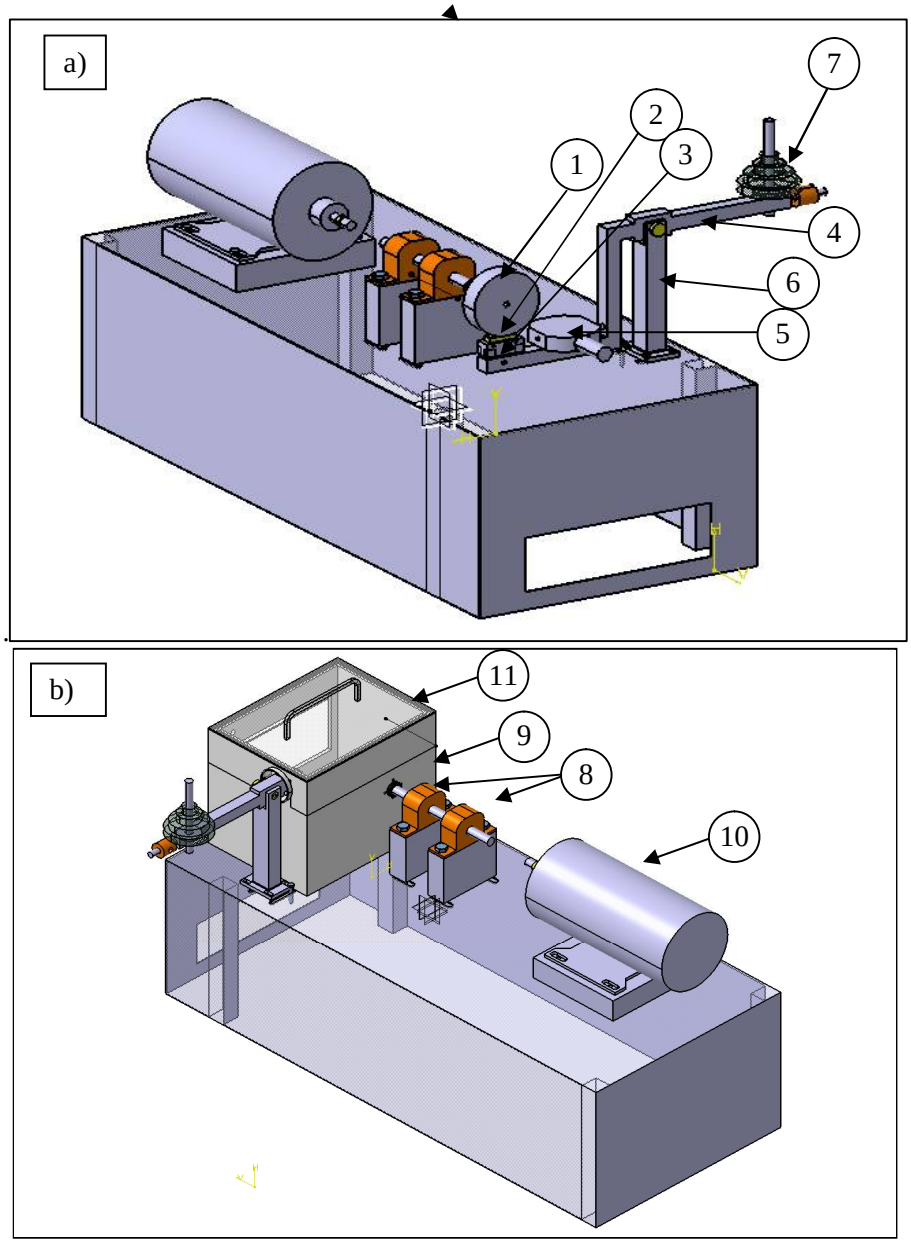

Figure 3.3: Three-dimensional view of the hybrid tribology machine

Notes. 1. Counterface stainless steel (AISI 304), 2 Sample, 3. Sample holder, 4. Lever, 5. Load cell, 6. Lever holder, 7. Weight (applied load), 8. Bearings, 9. Container cover, 10. 0.5 hp motor, 11. Oil container.

The frictional force was captured by a custom-made load cell immersed in the lubricant. The load cell was designed especially to work under this condition. It is able to work under temperatures up to 150^{o}C and any lubricant condition. A special load cell provided by Bestech Australia Pty Ltd was used in the machine, where it was fixed in a position that enable the measurement of the frictional force (Figure 3.4). It was specially designed to be operated at high temperature and lubricant conditions, and it was directly connected to a computer to capture the frictional force. The machine operated using a DC 0.5 hp motor working with 24 V power. This helped to control the sliding speeds using the data requisition system. The container was filled with new oil for each set of data.

ISSN(Online) : 2319-8753
ISSN (Print) : 2347-6710

International Journal of Innovative Research in Science, Engineering and Technology

(An ISO 3297: 2007 Certified Organization)

Website: www.ijirset.com

Vol. 6, Issue 2, February 2017

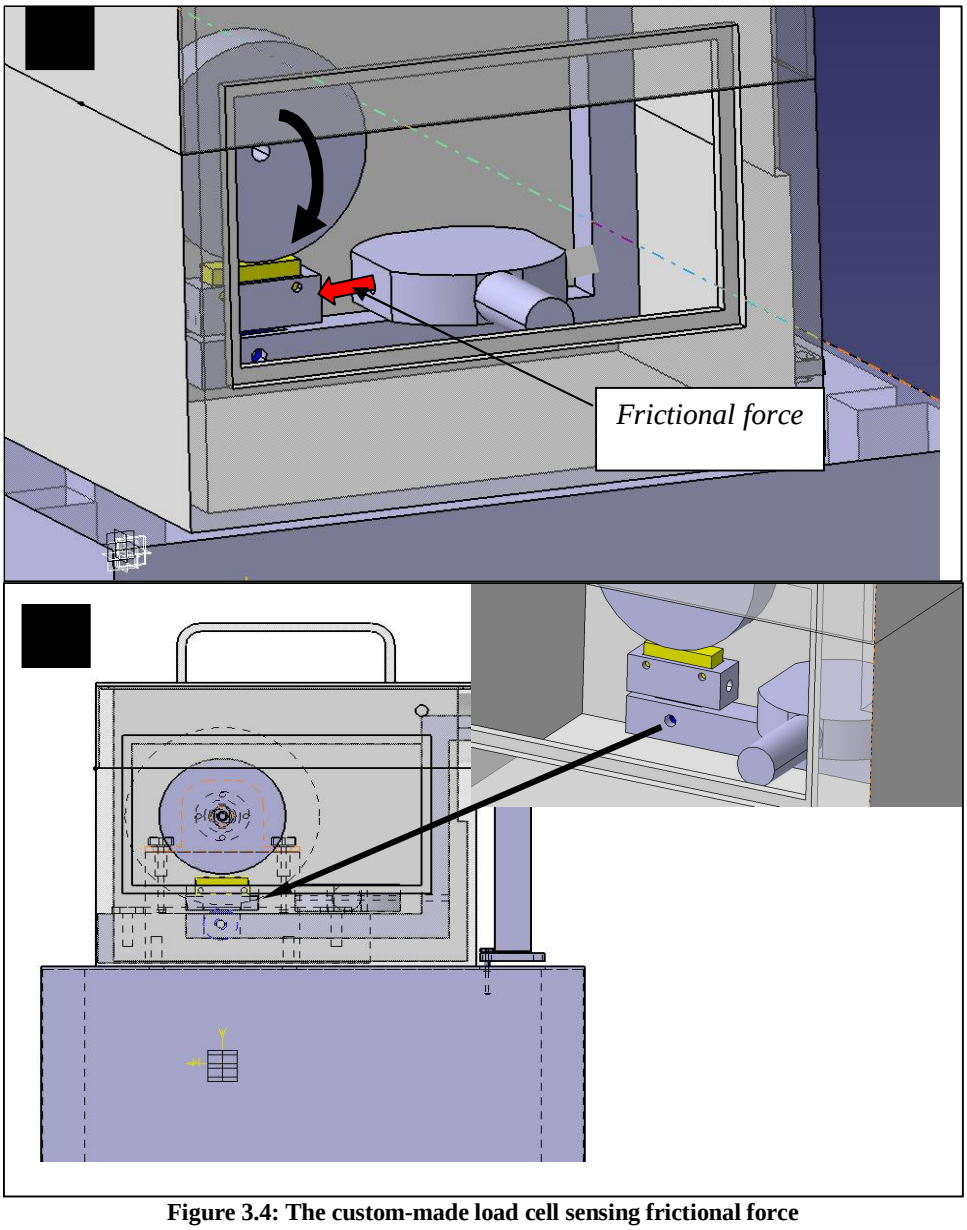

Figure 3.4: The custom-made load cell sensing frictional force

In the current design, the specimen was fully immersed in a lubricant container which represented the real implementation of the lubricant. In other studies, in which the main application of vegetable lubricants seems to be for ball bearings, the oil was applied through a pump onto the counterface [10, 11]. Those works may assist in understanding the tribological behaviour of the rubbed pair under lubricant condition but not the performance of the lubricant itself. In the current study, the sample was fully covered by the lubricant and the lubricant was allowed to penetrate in the interface freely, to represent its real application. To achieve such complicated environments, a sealing problem may occur. A heater was placed in the container to heat up the oil. In addition, a special window glass was designed to monitor the temperature distribution inside the container to observe the correlated interface temperature with the wear and frictional results.

ISSN(Online) : 2319-8753
ISSN (Print) : 2347-6710

International Journal of Innovative Research in Science, Engineering and Technology

(An ISO 3297: 2007 Certified Organization)

Website: www.ijirset.com

Vol. 6, Issue 2, February 2017

In light of this, a few leakage interactions were considered in the design and sealed well (Figure 3.5): the entrance of the lever, rotated shaft (coming from the motor), load cell wire, glass window, and cover of the container. A special sealing silicon (high-temperature RTV silicone, Loctitie) was used to seal of the load cell wire and the glass window associated with some bracket and screws to prevent any leakage of lubricant during the high speed of the counterface. For the cover of the container, a groove was machined at the top of the container and filled with a hydronic O-Ring seal (Fluorocarbon Elastomer O-Ring with a diameter of 4mm), which has high resistance to elevated temperature. To seal the hole of the shaft in the container, a hydraulic seal was used and a cup was designed to hold the seal firmly on the container wall (Figure 3.5b). For the entrance of the lever, a flexible rubber cover (Joint Boot Dust Shield Cover) was used to prevent any leakage of the oil from that entrance (Figure 3.5c).

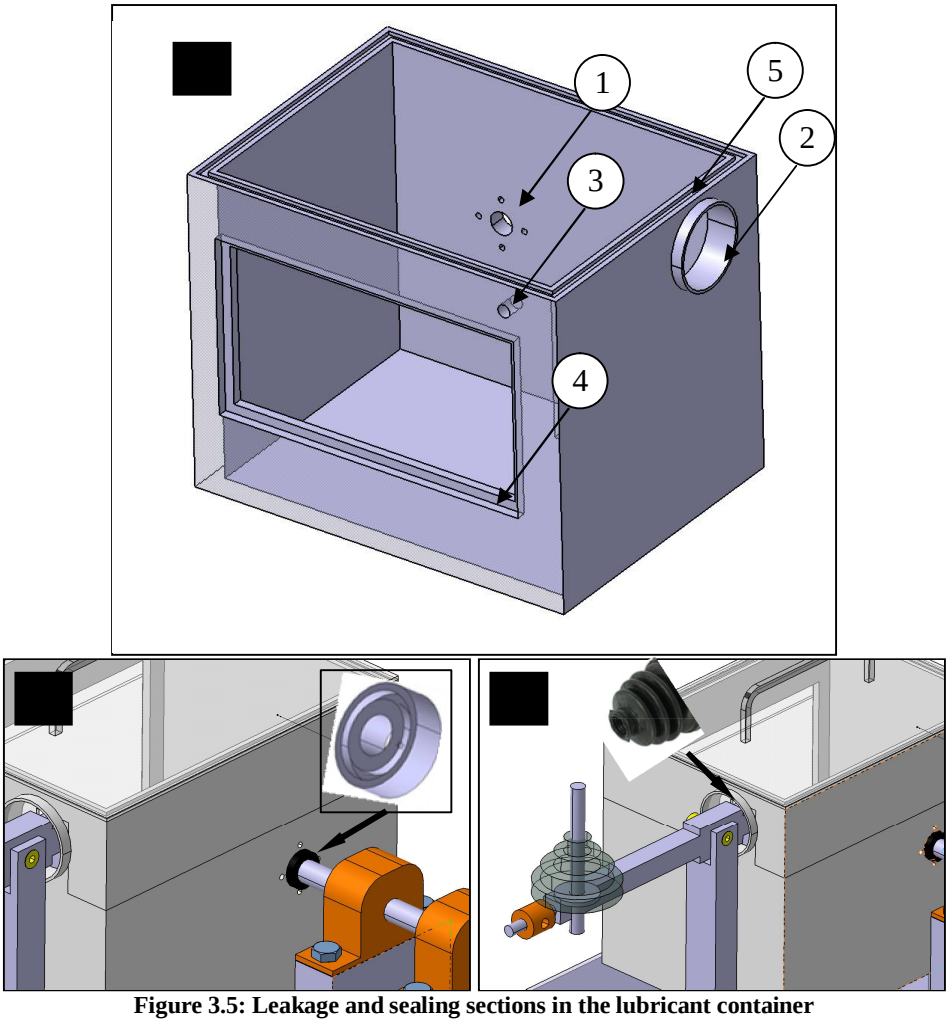

Figure 3.5: Leakage and sealing sections in the lubricant container

The machine was fabricated locally at the USQ workshop with the use of different CNC machines (Figure 3.6). Optimisation and reconsideration processes were undertaken after the fabrication. Some safety regulation standards were included in the design for authorisation purposes. First, a cover was needed for the coupling and shaft from the motor to the counterface in the container in case the operator mistakenly placed his or her finger on the shaft (Figure 3.6a). Moreover, emergency stop was required and placed above the power supplier. At this position, the emergency

ISSN(Online) : 2319-8753
ISSN (Print) : 2347-6710

International Journal of Innovative Research in Science, Engineering and Technology

(An ISO 3297: 2007 Certified Organization)

Website: www.ijirset.com

Vol. 6, Issue 2, February 2017

stop is easy to find, and close to the operator in case of emergencies (Figure 3.6 b). To avoid any leakage during the operating process, all the seals were placed and then checked (Figure 3.6c).

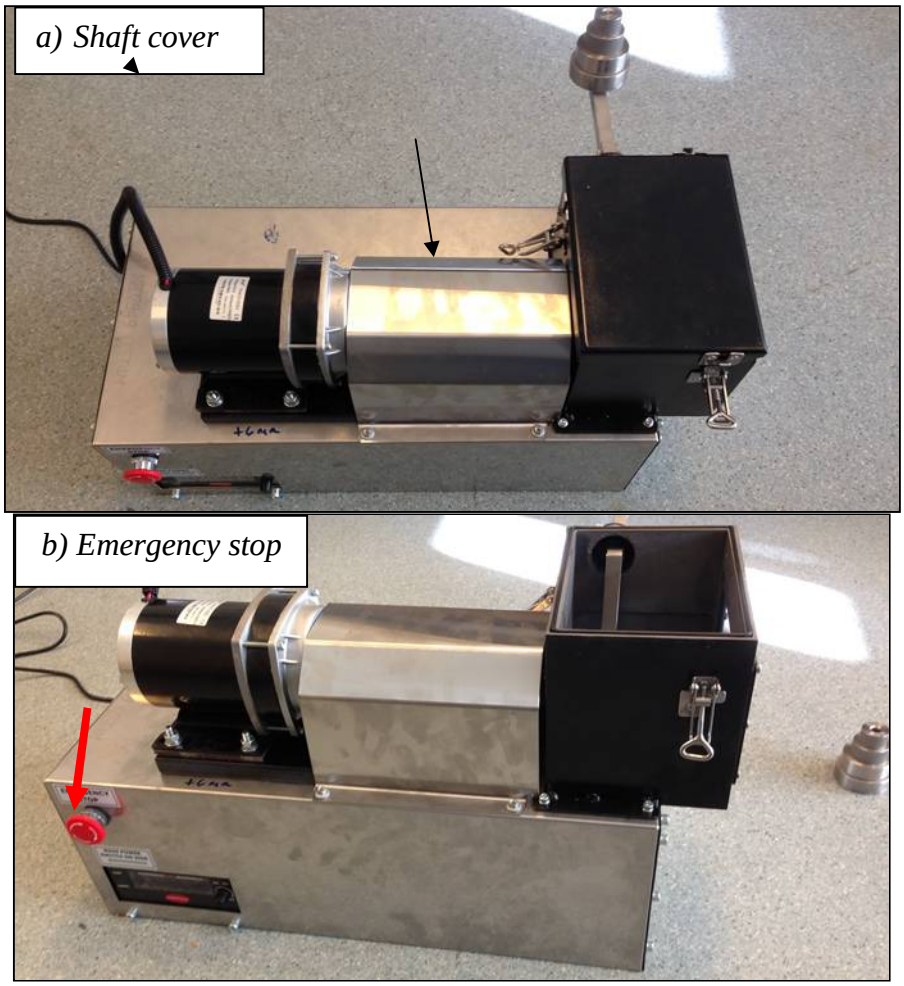

ISSN(Online) : 2319-8753
ISSN (Print) : 2347-6710

International Journal of Innovative Research in Science, Engineering and Technology

(An ISO 3297: 2007 Certified Organization)

Website: www.ijirset.com

Vol. 6, Issue 2, February 2017

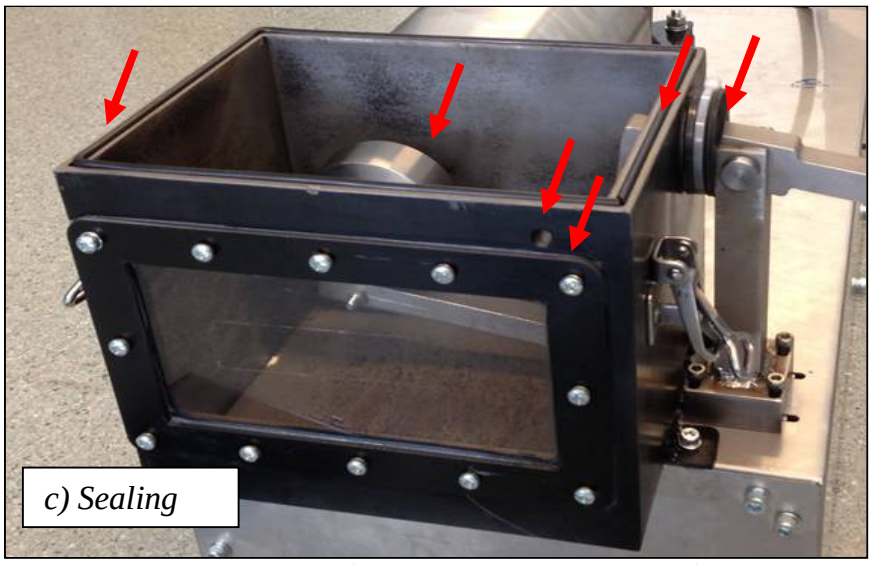

Figure 3.6: Assessment stage of the hybrid tribology machine before operation

Figure 3.7 displays the machine under the operating condition of the lubricant, showing the capture of the frictional force with the presence of the lubricant in the container and monitoring the heat distribution in the container using the thermo-imager.

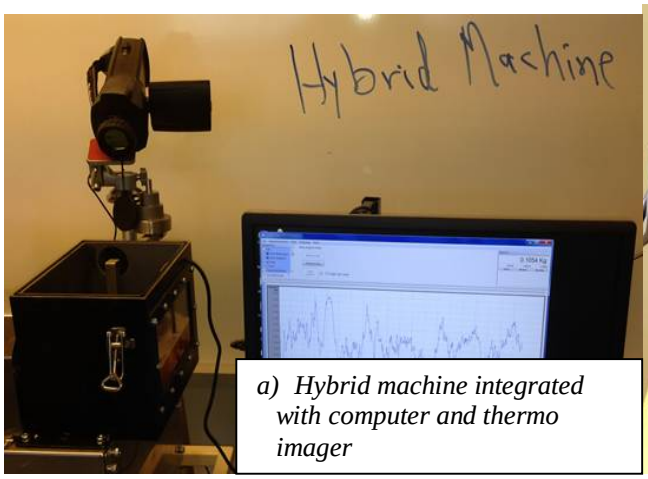

a) Hybrid machine integrated with computer and thermo imager

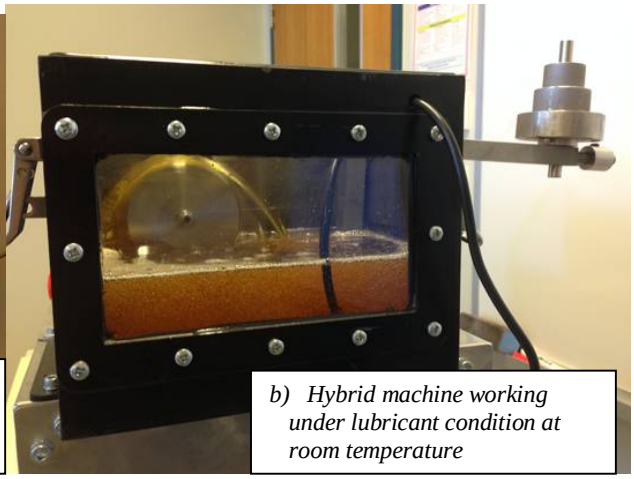

b) Hybrid machine working under lubricant condition at room temperature

ISSN(Online) : 2319-8753
ISSN (Print) : 2347-6710

International Journal of Innovative Research in Science, Engineering and Technology

(An ISO 3297: 2007 Certified Organization)

Website: www.ijirset.com

Vol. 6, Issue 2, February 2017

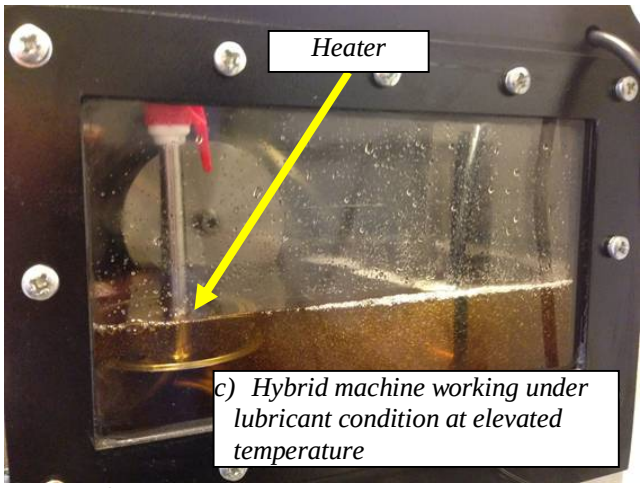

Figure 3.7: Photos of the hybrid tribological machine integrated with the computer

III. VERIFICATION OF THE NEW HYBRID TRIBOLOGICAL MACHINE

For verification of the new hybrid machine and establishing datum data, dry tests were conducted using the newly designed machine under the same pressure and sliding speed as those used with the laboratory machine (Chapter 4 and Section 3.4.1). The pressures used for the laboratory machine were 38 kPa, 90kPa and 113.7kPa at a sliding speed of 2.8m/s. The pressure was determined based on the applied load divided by the worn surface after the tests. 113.7 kPa was used for the verification, which was equivalent to the applied load of 1.13 kg at similar speed of 2.8m/s of the laboratory machine.

The specific wear rate *(SWR)* of the selected metals was determined using equation (3.1):

$$SWR = \frac{\Delta w / \rho}{L \times D} \tag{3.1}$$

where the Δw is weight difference (before and after the test) which will be determined using a very high precision weight scale, ρ is the density of the materials, L is the applied load, and D is the sliding distance.

The results of the specific wear rate of three tests for each condition are predicted in Figure 3.8 for all the materials using both the laboratory and new hybrid machine. Both results were close and the error percentage was less than 5%, which could be due to the complexity of the experiments.

ISSN(Online) : 2319-8753
ISSN (Print) : 2347-6710

International Journal of Innovative Research in Science, Engineering and Technology

(An ISO 3297: 2007 Certified Organization)

Website: www.ijirset.com

Vol. 6, Issue 2, February 2017

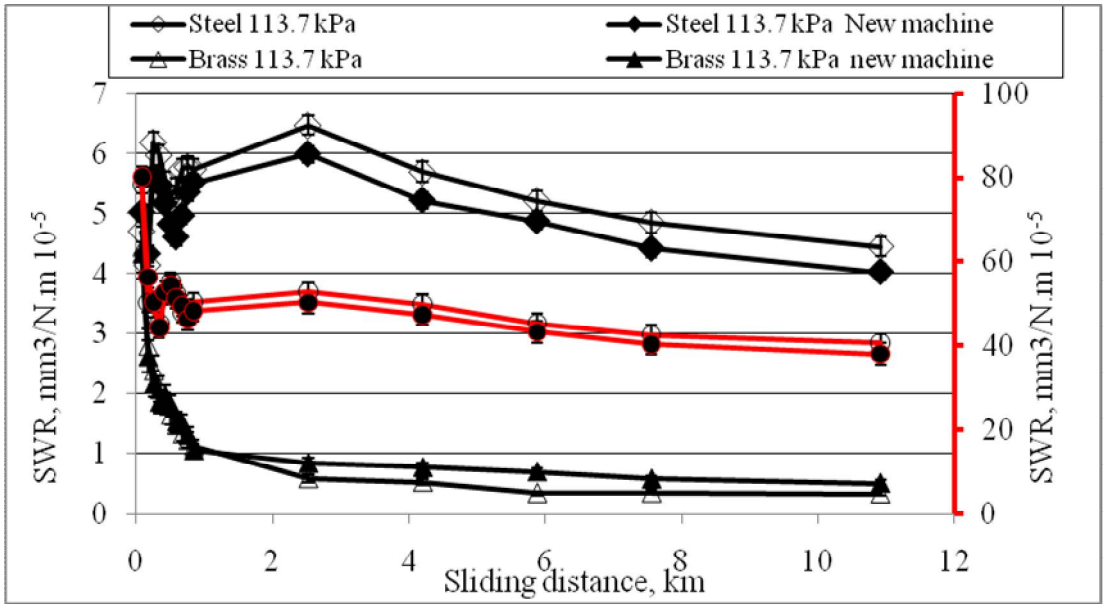

Figure 3.8: Specific wear rate of the selected materials at 113.7 kPa applied stress using the new hybrid and laboratory machines at 2.8m/s sliding distance

IV. EXPERIMENTAL PROCEDURE

The experiments were divided into two categories. At the initial stage, dry adhesive wear testings were performed using the available tribology machine at USQ (Yousif [9]. The machine is able to conduct several tribological tests. With this machine, the first category of the testing was conducted (i.e. comprehensive evaluation of the dry adhesive wear behaviour of common metals). But, the machine is not capable of using lubricants at elevated temperatures. Therefore, in the second category, the adhesive wear testing under lubricant conditions was conducted using the newly designed tribological machine (hybrid machine). In the following sections, both dry and lubricant testings are explained.

I. DRY ADHESIVE WEAR TESTING

For the experiments, adhesive wear tests were conducted against a stainless steel ring (AISI 304) using the BOR technique according to the ASTM G77-98 [12] (Figure 3.9). The machine was equipped with a load cell to capture the frictional force during sliding. The sample (3) was fixed to the holder, which was placed on a ball bearing to gain the minimum frictional contact. Calibration was made for each set of testing and the average of the results reported. Further information about the machine can be found in Yousif [9].

ISSN(Online) : 2319-8753
ISSN (Print) : 2347-6710

International Journal of Innovative Research in Science, Engineering and Technology

(An ISO 3297: 2007 Certified Organization)

Website: www.ijirset.com

Vol. 6, Issue 2, February 2017

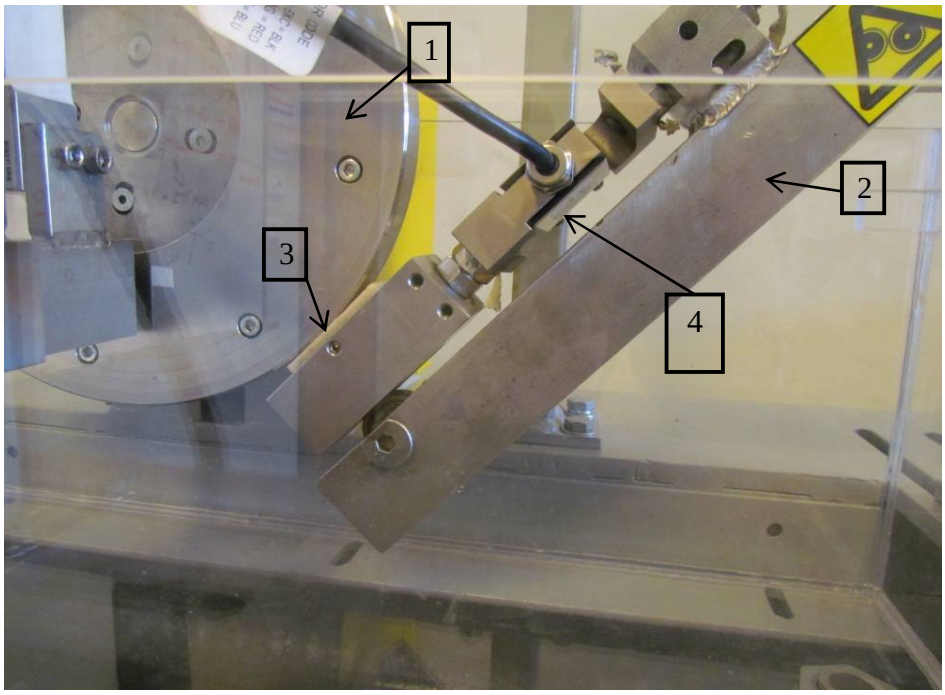

Figure 3.9: Tribological machine with block-on-ring configuration (Yousif [9]

Notes. 1. Counterface, 2. BOR load lever, 3. Specimen, 4. Load cell.

To ensure intimate contact between the sample and the counterface, before each test the disc was polished with abrasive SiC paper (G1500) to a surface roughness of 0.1-0.3 μm Ra. Acetone was used to clean the surface before each test, followed by wet cotton to remove the acetone and clean the surface. The samples were polished before each test and the roughness of their surfaces was measured. The roughness of the samples were about 0.075μm Ra, 0.4 μm Ra, and 0.25 μm Ra for mild steel, aluminium and brass, respectively (Figure 3.10).

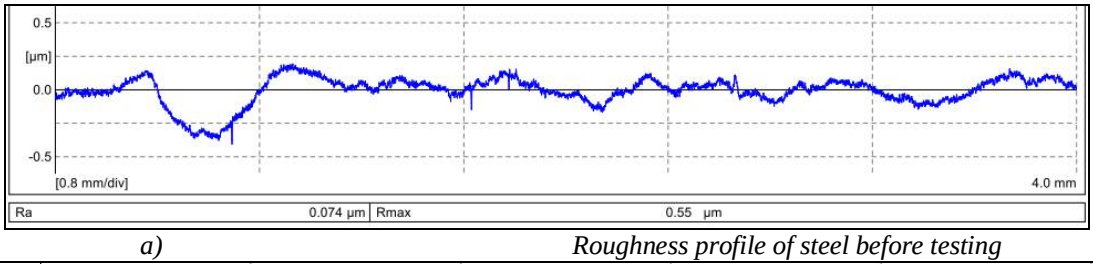

a) *Roughness profile of steel before testing*

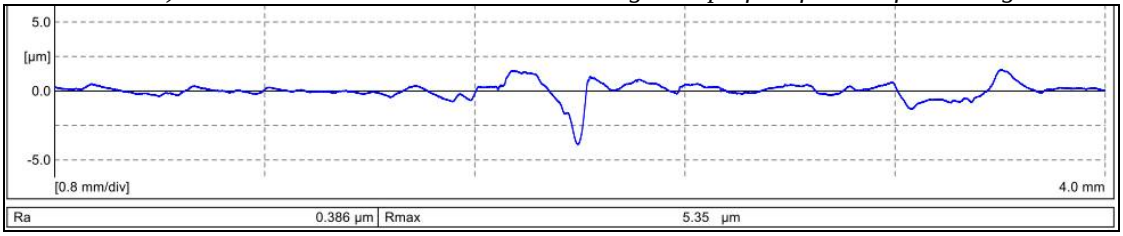

b) *Roughness profile of aluminium before testing*

ISSN(Online) : 2319-8753
ISSN (Print) : 2347-6710

International Journal of Innovative Research in Science, Engineering and Technology

(An ISO 3297: 2007 Certified Organization)

Website: www.ijirset.com

Vol. 6, Issue 2, February 2017

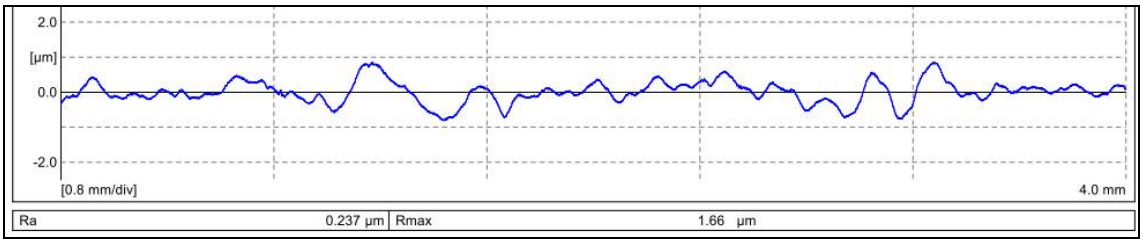

c) *Roughness profile of brass before testing*

Figure 3.10: Roughness profiles of sections on the polished samples before testing* ***the scale of the figures are different since they are auto-generated by Mahr roughness machine.***

Sliding tests were conducted at ambient temperature and humidity conditions with various normal loads (30 N, 40 N and 50 N), and sliding distances (0–10.8 km) and sliding speed of 2.8 m/s. It is known that each material has its own pressure x velocity limit. For the current study, preliminary experiments were conducted to determine the PV limits of the selected metals and gain the optimum velocity, with a constant applied load of 50 N. 2.8 m/s sliding velocity was found to be the optimum for the three selected metals considering different applied loads. The normal applied loads were equivalent to 38 kPa, 90kPa and 113.7kPa which were calculated after the test by dividing the applied load by measuring the worn surface area. Surface morphology and collected debris were examined after each test using a scanning electron microscopy. A Mahr roughness profile machine was used to determine the roughness of the rubbed surfaces after each test. The roughness was measured against the sliding direction for both the metal surfaces and the counterface. The sample, counterface, interface and environmental temperatures were monitored using a thermo-imager device.

Friction coefficient μ is calculated using equation (3.2) where F_f is the frictional force which is captured via the load cell and L is the applied load:

$$\mu = \frac{F_f}{L} \tag{3.2}$$

II. ADHESIVE WEAR TESTING UNDER LUBRICANT CONDITION

The newly designed machine was used to conduct wear testing under the lubricant condition. The first step in the experiments was to prepare the sample and counterface similar to the preparation process explained in Section 3.4.1.

WCO blends, WCO:SO of 0 vol. %, 25 vol. %, 50 vol. %, 75 vol. % and 100 vol. % were used in the current study. Several steps had to be considered in conducting the experiments. At the initial stage, the specimens were polished, weighed and then fixed in the holder of the hybrid machine. The lever of the machine was loaded with the required dead weight. The lubricant container was filled with the lubricant to a level of about 30 mm above the specimen to ensure that the specimen was fully immersed in the lubricant during the test. To avoid lubricant splash during the experiments, the container was firmly covered. Then the heater was switched on to the required temperature. The panel controller was set to the required rotational speed and the load cell reader and timer was set to zero. The machine was then switched on and, when the required time was reached, it was switched off.

At the end of each test, it was important to wait for the lubricant to cool down and then clean the lubricant container by vacuuming it using the oil pump and then filter the oil and extract the debris. The specimen was removed and cleaned with acetone. Weight and surface roughness of the specimens were determined after the test was completed. The direction of the roughness measurement was perpendicular to the sliding direction. The lubricant container was cleaned

ISSN(Online) : 2319-8753
ISSN (Print) : 2347-6710

International Journal of Innovative Research in Science, Engineering and Technology

(An ISO 3297: 2007 Certified Organization)

Website: www.ijirset.com

Vol. 6, Issue 2, February 2017

with acetone to remove any residual oil after each set of tests. Frictional force was saved on the computer during the experiments.

Different sliding distances were used in the study to differentiate between the running-in and steady state regions (0 - 10.8 km). The operating conditions and parameters are given in Table 3.3. For each test, at least three repetitions were conducted and the average of the results was determined. Since the dry tests were conducted at the speed of 2.8 m/s, the lubricant tests were conducted at the same speed for comparison purposes.

Lubricant tests were conducted against a stainless steel ring (AISI 304) and, to ensure intimate contact between the sample and the counterface, before each test the disc was polished with abrasive SiC paper (G1500) to a surface roughness of 0.1-0.3 μm Ra, i.e. the three metals were tested on an identical surface characteristic. This ensured that the wear and frictional data of the three different metals were comparable under the same contact and operating conditions. Acetone was used to clean the surface before each test, followed by wiping wet cotton to remove the acetone and clean the surface. The specimens were machined from a block of the metals, and before the tests the specimens were polished. The roughness of the samples were about 0.075μm Ra, 0.4 μm Ra, and 0.25 μm Ra for mild steel, aluminium and brass, respectively (Figure 3.10). A Mahr roughness profile machine was used to determine the roughness of the rubbed surfaces before and after each test. The roughness was measured against the sliding direction for both the metal surfaces and the counterface.

Table 3.3: Operating Parameters for Adhesive Wear Testing under Lubricant Conditions

Duration, min	Applied load, N	Oil temperature, ^{o}C
15	5	30
30	10	40
45	15	60
60	20	80
15	5	30
30	10	40
45	15	60
60	20	80
15	5	30
30	10	40
45	15	60
60	20	80
15	5	30
30	10	40
45	15	60
60	20	80

At the end of the lubricant tests, the debris was collected and extracted for scanning electron microscope (SEM) observation. In the extraction, the debris was immersed in the oil and then collected in small tubes (Figure 3.11). A centrifuge machine was used to extract the debris at the first stage of oil separation. The lubricated debris was washed more than five times with acetone and then centrifuged. A hot air dryer was used to dry the debris. The collected debris was attached to a conducted carbon tap for the SEM observation.

ISSN(Online) : 2319-8753
ISSN (Print) : 2347-6710

International Journal of Innovative Research in Science, Engineering and Technology

(An ISO 3297: 2007 Certified Organization)

Website: www.ijirset.com

Vol. 6, Issue 2, February 2017

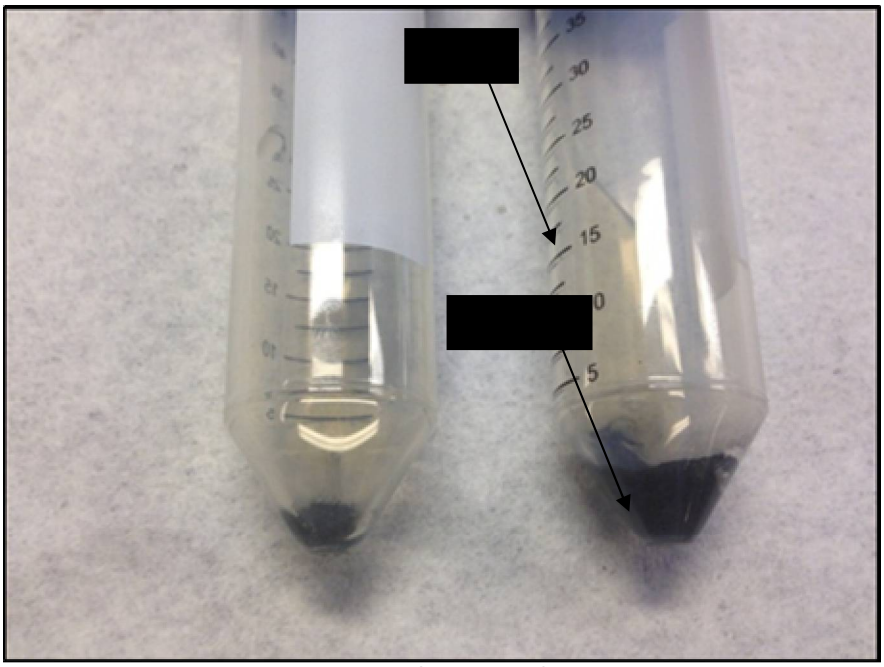

Figure 3.11: Extraction of the debris from the lubricant

Different oils were used in this work, and these were supplied by Shell Helix. The technical data for each oil grade is provided by the company via http://www.shell.com/global/products-services/on-the-road/oils-lubricants. Some specific details of the selected oil are given in Table 3.4. The main conventional oil used in the work is 5W-30 which is fully synthetic (as determined by Shell Helix).

Table 3.4: Some of the fully synthetic oil specifications

	MRV, ASTM D4684	Density, ASTM D4052	Flash point, ASTM D92	Pour point, ASTM D97	Remarks
5w-30	17000	852	240	-48	fully synthetic
5w-40	19300	840.3	242	-45	fully synthetic
10w-50	21500	862.3	235	-41	fully synthetic
15w-40	26100	882	230	-33	multi-grade

V. PROPERTIES OF WASTE COOKING OIL

A. POUR POINT AND FLASH POINTS

Pour point is one of the important properties of oil since it represents the characteristics of the oil at the condition in which it becomes semi solid and not able to flow. The ASTM D 97 standard is used in this study and has been adopted by many researchers [13]. In the test, a pour point tester was adopted with a cooling system working with methanol as the cooling agent. 45 ml of the blend was placed in a test jar and the level of the liquid marked. The jar of the blend then began cooling to about -40^{o}C using the pour testing apparatus. While the blend was cooling, the movement of the

ISSN(Online) : 2319-8753
ISSN (Print) : 2347-6710

International Journal of Innovative Research in Science, Engineering and Technology

(An ISO 3297: 2007 Certified Organization)

Website: www.ijirset.com

Vol. 6, Issue 2, February 2017

blend and pour point was observed. Once the blend solidified, it was placed on the apparatus horizontally to heat up at atmospheric condition, the temperature was taken with each 3°C drop, and the flow of the blend was observed until the first droplet fell. This process was repeated three times for each blend. The results are presented in Table 3. 5. It is clear that the pour point of the WCO is greater than the SO and WCO blends. This has also been reported for rapeseed oil [14]. Quinchia, Delgado [14] recommended that vegetable oil-based lubricants may need lower their pour point temperatures for some applications such as hydraulic fluids, chain saw oils and saw mill oils. Similarly, for such applications, it is recommended that PPD additives are considered to assist in delaying the nucleation and crystal growth stages of the oil [15].

The flash point can be defined as the lowest temperature at which the oil forms an explosive vapour under normal atmospheric conditions. A Cleveland open cap tester was used to determine the flashpoint according to ASTM D92. The average of the flash point of the blends is given in Table 3.4. In general, the higher the flash point the better. In comparing the WCO and the SO, the flash point of the WCO is greater, which can be an advantage. All the research related to WCO aimed to investigate the performance of the biofuel extracted from the WCO [16, 17]. In these works, it was highly recommended to reduce the flash point to about 150°C by using ferric sulfate and potassium hydroxide as catalysts in a two-step reaction.

Table 3.5: Pour Point and Flash Point of the Blends

Blend	Pour point	Flash point
0% SO	-16 °C ± 1.25	285 °C ± 8
25% SO	-22 °C ± 1.5	275 °C ± 6
50% SO	-26 °C ± 1.7	243 °C ± 6
75% SO	-30 °C ± 1.9	236 °C ± 5
100% SO	-36 °C ± 0.75	225 °C ± 5

B. VISCOSITY OF THE WASTE COOKING OIL AND ITS BLENDS

The dynamic viscosity of the used oil and its blends against different temperatures is plotted, in two forms, in Figure 3.12. It has been mentioned here that the results in the figures are presented for unused waste cooking oil (before cooking), after filtering (cooked and filtered), and prepared blends of waste cooking oil with the 5% (wt) of EVA copolymer and 2% (wt) of EC and the synthetic oils. The figures show that there is a dramatic increase in the viscosity of the waste cooking oil with the addition of the additives and further increase achieved with the addition of synthetic oil. In other words, the unused waste cooking oil (cotton seeds) exhibits very low viscosity and cooking it with fish and chips slightly increase the viscosity. The addition of the 5% (wt) of EVA copolymer and 2% (wt) of EC significantly impacts the viscosity behaviour of the oil as the waste oil becomes competitive especially at higher temperature. Such improvement will dramatically impact the tribological performance of the oil.

ISSN(Online) : 2319-8753
ISSN (Print) : 2347-6710

International Journal of Innovative Research in Science, Engineering and Technology

(An ISO 3297: 2007 Certified Organization)

Website: www.ijirset.com

Vol. 6, Issue 2, February 2017

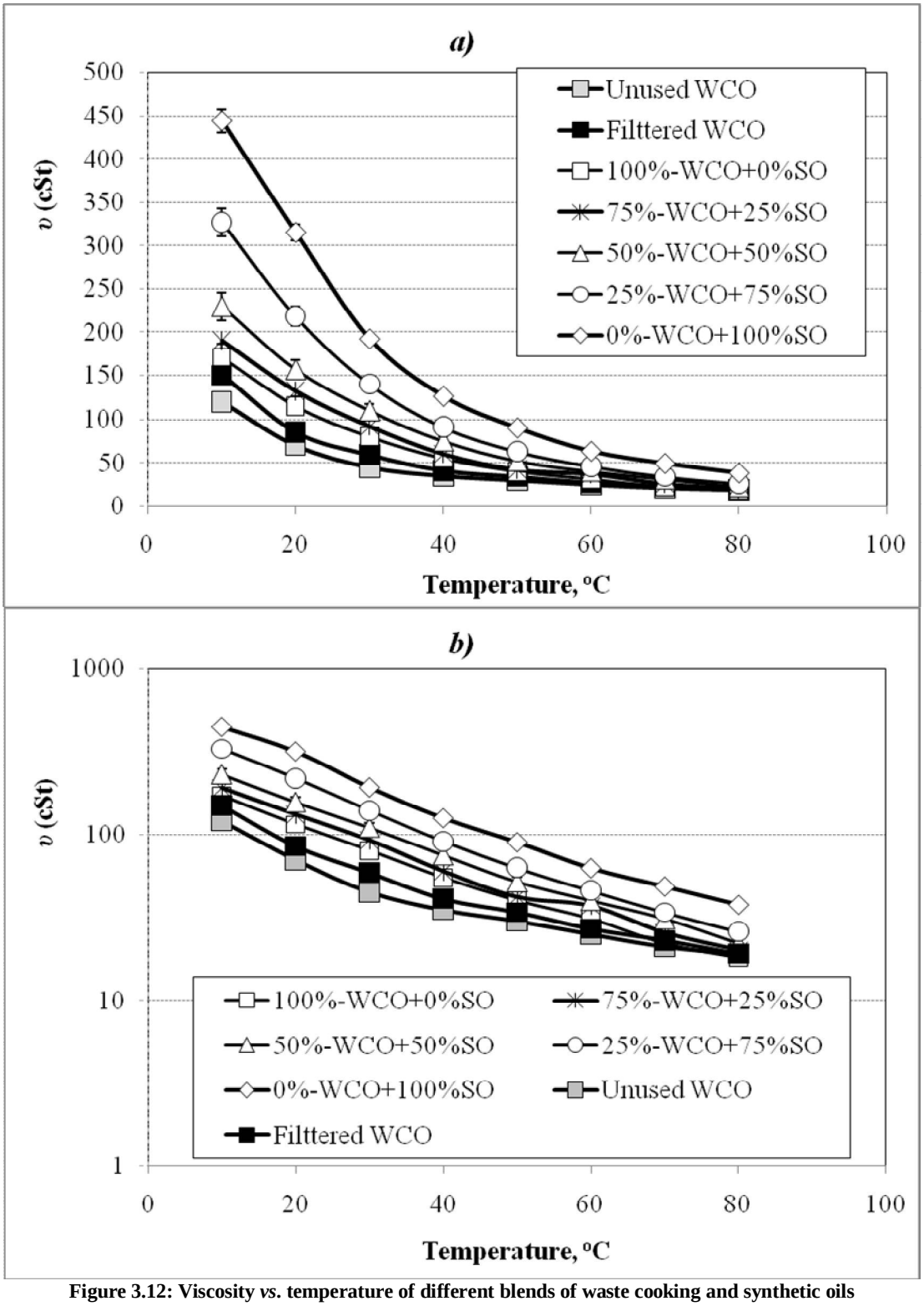

Figure 3.12: Viscosity *vs.* temperature of different blends of waste cooking and synthetic oils

ISSN(Online) : 2319-8753
ISSN (Print) : 2347-6710

International Journal of Innovative Research in Science, Engineering and Technology

(An ISO 3297: 2007 Certified Organization)

Website: www.ijirset.com

Vol. 6, Issue 2, February 2017

Some of the data in the literature is presented in log form [18] and for comparison purposes the current values are presented in these two forms. The general trend of the viscosity decreases with increases in the temperature as this is expected for all the types of oil. For the 0% blend of WCO (fully synthetic) there was approximately 900% drop in viscosity when the temperature was increased from 10°C to 80°C. Meanwhile, the drop in viscosity of the pure WCO was about 600%. These results are promising for WCO in terms of stability and less sensitivity to temperatures compared to synthetic oil. A similar trend can be seen in Figure 3.12b.

It is well known that the determination of oil application and performance is based on viscosity at 40°C and 80°C. Therefore, the viscosities of the blends at those temperatures are extracted from Figure 3.12 and presented in Figure 3.13. It is obvious that SO has higher viscosity values compared to its blends. Moreover, the increased addition of WCO reduces the viscosity of the blends for both selected temperatures (Figure 3.13).

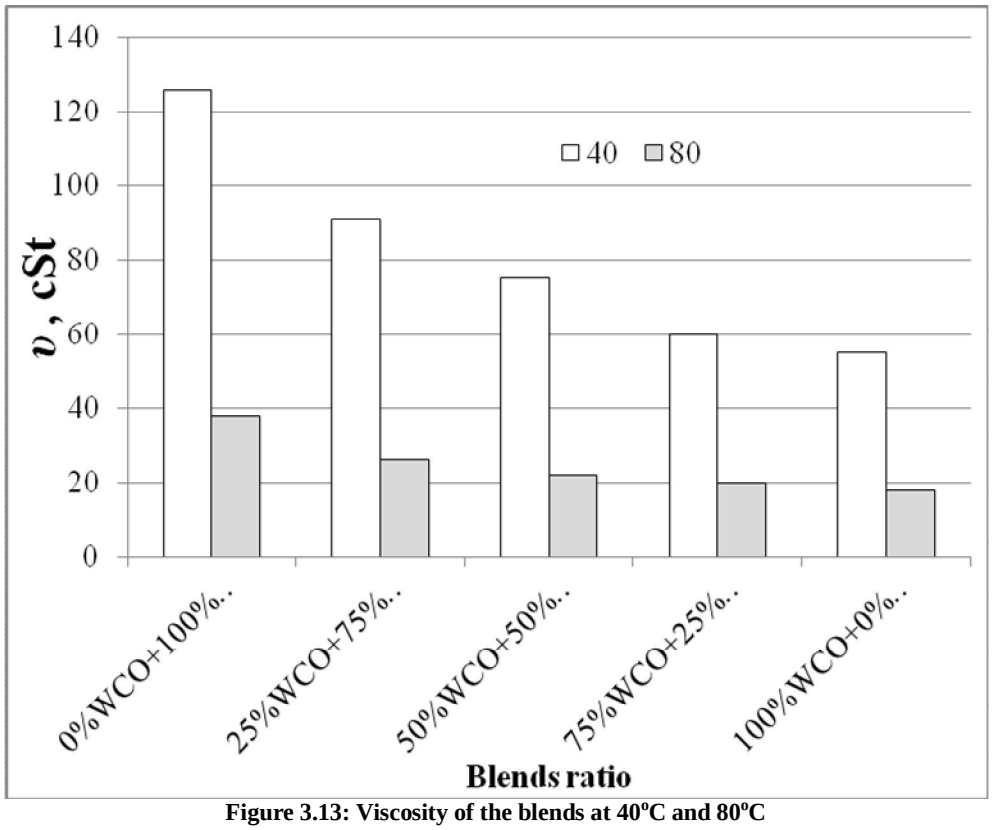

Figure 3.13: Viscosity of the blends at 40°C and 80°C

The ISO viscosity grade requirements are listed in Table 3.6. For the current blends it can be seen that pure WCO can fit with the ISO VG 68, which can be used for crankcase oil grades 20 W [19, 20]. However, further study is required to determine the degradability of the oil and the tribological performance of the components under this lubrication condition.

ISSN(Online) : 2319-8753
ISSN (Print) : 2347-6710

International Journal of Innovative Research in Science, Engineering and Technology

(An ISO 3297: 2007 Certified Organization)

Website: www.ijirset.com

Vol. 6, Issue 2, February 2017

Table 3.6: ISO Viscosity Grade Requirements [21-23].

Kinematic viscosity	ISO VG32	ISO VG46	ISO VG68	ISO VG100	Pure waste cooking oil
@40 °C	>28.8	>41.4	>61.4	>90	65.5
@100 °C	>4.1	>4.1	>4.1	>4.1	9.5

Further to the above and since there are few studies on the WCO as a lubricant, the viscosity of different grades of oils were tested and compared with those of WCO (Figure 3.14). In general, WCO exhibits the lowest viscosity compared to other SOs. This can be both an advantage and disadvantage since low viscosity means less resistance to the shear (low friction) and less film thickness in the interface when two bodies are under sliding condition. Nevertheless, one can see that the pure WCO is close to the W5-30 oil. The W5-30 fully synthetic oil is recommended for both gasoline and diesel engines. However, the viscosity index must also be considered to determine the application of the oil.

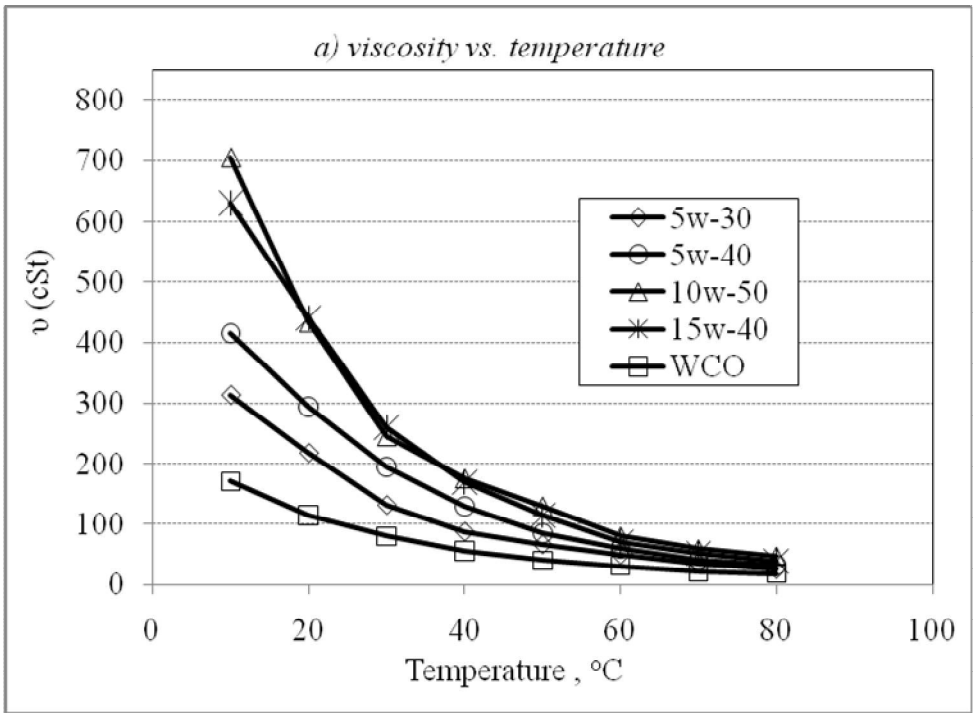

ISSN(Online) : 2319-8753
ISSN (Print) : 2347-6710

International Journal of Innovative Research in Science, Engineering and Technology

(An ISO 3297: 2007 Certified Organization)

Website: www.ijirset.com

Vol. 6, Issue 2, February 2017

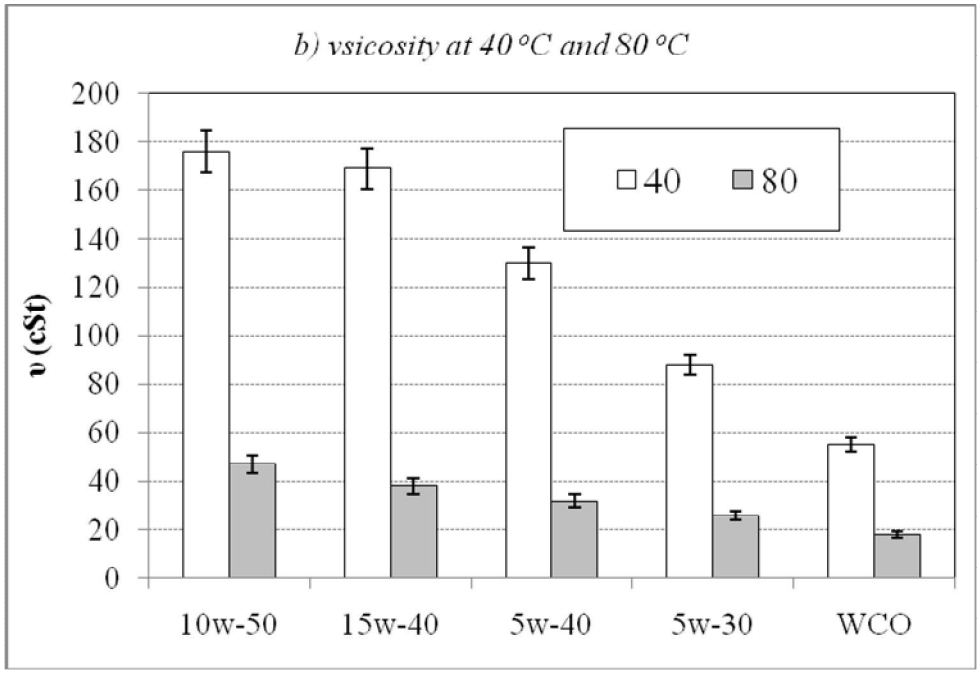

Figure 3.14: Waste cooking oil viscosity with industrial lubricant

The viscosity index of WCO and its blends were determined by measuring the viscosity of the lubricant at an elevated temperature of 100°C. The results are presented in Figure 3.15. It seems there is a significant deterioration in the viscosity of the WCO. In this work, 5% (wt) of EVA copolymer (density, at 23 °C, 0.956 g cm-3; molecular weight, 60250 g mol-1; melting temperature, 59 °C) and 2% (wt) of EC (density, at 25°C, 1.14 g cm-3; molecular weight, 68960 g mol-1; melting temperature, 155°C) were used as additives to enhance viscosity at high temperature. The advantages of the EVA are that it is an inert, non-toxic and stable material, not expected to be biodegradable and not hazardous [24]. EC is a kind of water-insoluble cellulose ether having good mechanical properties, relatively low cost and good film-forming performance [25]. The addition of the additives significantly improved the viscosity index of all the WCO blends, making it comparable to the fully synthetic oil of 5W-30 (≈ 155). The blends with the additives were used in the journal bearing tests presented in Chapter 6.

ISSN(Online) : 2319-8753
ISSN (Print) : 2347-6710

International Journal of Innovative Research in Science, Engineering and Technology

(An ISO 3297: 2007 Certified Organization)

Website: www.ijirset.com

Vol. 6, Issue 2, February 2017

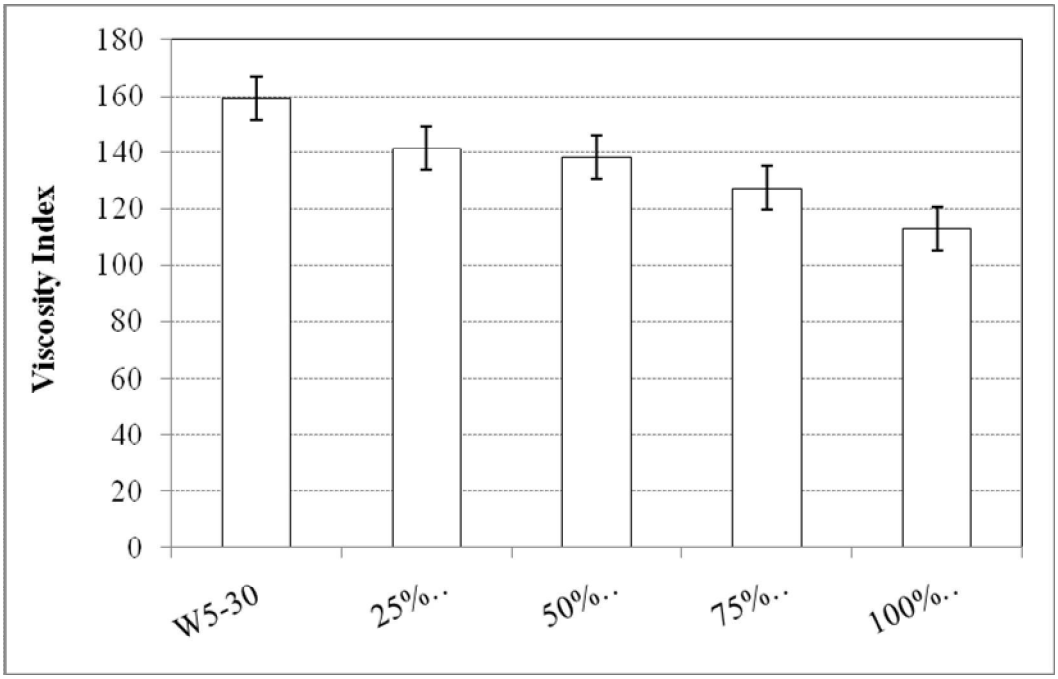

Figure 3.15: Viscosity index of waste cooking oil and its blend with W 5-30

The use of some vegetable oils as a potential lubricant has been investigated in previous studies, the most recent of which are summarised in Table 3.7. These show the viscosity of vegetable oils at 40°C and 80°C. There are different ranges of viscosity for the oil and there could be comparable values for the pure WCO with soybean and sunflower oil [26], even though WCO exhibits a better viscosity value. In [27], a modifier was used to improve the viscosity performance of the vegetable oil, and this can be considered for future work on WCO.
Some important points can be drawn from this literature as follows:

- There is a growing environmental need to find alternative lubricants, and a great deal of research has focused on the possibility of using vegetable oils. Inedible rather than edible oils is highly recommended.
- The disposal of WCO is an issue. WCO's potential as an alternative fuel for diesel engines has been explored, but it is limited as a fuel; because it impacts substantially on engine performance from a tribological perspective.
- The potential of using WCO as an alternative lubricant was investigated in the current study. From a viscosity point of view, there are promising results regarding its use as a lubricant, but further study is recommended.

ISSN(Online) : 2319-8753
ISSN (Print) : 2347-6710

International Journal of Innovative Research in Science, Engineering and Technology

(An ISO 3297: 2007 Certified Organization)

Website: www.ijirset.com

Vol. 6, Issue 2, February 2017

Table 3.7: Comparison to Previous Works and Standards

	υ (cSt) at 40 ^{o}C	υ (cSt) 80 ^{o}C
0	126	38
25	94	26
50	75	22
75	60	20
100	55	18
Original soybean [18]	≈ 175	≈ 29
Jatropha oil [10]	≈ 172	≈ 23
Soybean oil [24, 26]	33.6 ± 0.9	12.3 ± 0.5
Sunflower oil [24], [26]	32.9 ± 2.3	12.7 ± 0.8
Castor oil [24, 26]	242.5 ± 21.7	37.1 ± 1.7
Castor seeds [28]	248.8	NA
Iluent (polyalphaolefin), and high-oleic vegetable oils [29].	42.33	
BIO-H01 is a mixture of 83.5% high oleic sunflower oil and 13.5% ditridecyl adipate [27]	37.41	11.42
BIO-H02 blend of high oleic sunflower oil at 73% and 24% of disooctyl adipate [27]	27.67	9.08

Influence of the Lubricant Temperature on the Wear and Friction Behaviour of the Metals

In this section, the specific wear rate, frictional coefficient, micrographs of the worn surfaces, roughness of the worn surface and debris morphology are presented when the experiments were performed under different lubricant temperatures. It should be mentioned here that these tests were conducted with a sliding distance of 10.8 km only under the applied load of 40 N, which can be considered to be a steady state.

ISSN(Online) : 2319-8753
ISSN (Print) : 2347-6710

International Journal of Innovative Research in Science, Engineering and Technology

(An ISO 3297: 2007 Certified Organization)

Website: www.ijirset.com

Vol. 6, Issue 2, February 2017

A. WEAR BEHAVIOUR

The influence of the different lubricant temperatures on the specific wear rate of the brass, aluminium and mild steel are presented in Figure 5.20 considering three different temperatures: 22^{o}C (room temperature), 40^{o}C and 80^{o}C. In general, one can see that the increase in the lubricant temperature increased the specific wear rate for all the materials. The main reason for the increase in the specific wear rate with the increase of the temperature is the reduction in the viscosity of the lubricant with the temperature increase (see Figure 3.13). The presence of the low-viscosity lubricant in the interface may help to clean the interface area but not separate the rubbed bodies completely, as seen in Figure 5.14. Ciantar, Hadfield [30] reported that low-viscosity oils resulted in severe wear since there is material transfer between the asperities and worn materials increase. This has also been concluded by Velkavrh and Kalin [31] and Imran, Masjuki [32] when the tests were conducted at different lubricant viscosity. The current study highlights that the temperature of the same lubricant impacts the wear performance. In addition to the viscosity modification due to the environmental temperature leading to an increase in the interaction between the asperities, the low viscosity of the oil helps to clean the interface from the worn debris. This could have advantages or disadvantages since washing out the debris will prevent the presence of the third body reported in Figure 4.13. Conversely, the washing out of the debris from the interface prevents film formation (plastic deformation on the rubbed surface), which in turn increases the removal of the material and decreases the stability of the surface characteristics. In other words, there are two occurrences that may assist in understanding the increase of the specific wear rate with the increase of the environmental temperature (reducing the viscosity): the continuation of modifications on the rubbed surfaces and the low separation of the two rubbed bodies. Observations of the SEM and the roughness of the worn surface will assist further and is discussed in the next sections.

Figure 5.21 displays the percentage increments in the specific wear rate due to an increase in the environmental temperature. It seems that the material most sensitive to the changes in the lubricant temperature is the aluminium compared to the brass and the mild steel. However, from Figure 4.4, the specific wear rate of the aluminium was much higher than the 14 10^{-5} mm^{3}/N.m under dry contact conditions, i.e. the presence of any type of the oil at high temperature of 80^{o}C reduces the specific wear rate by more than four times. Under dry contact conditions, the high heat in the interface associated with the third body (Figure 4.14) significantly damaged the surface of the aluminium. Despite the environmental temperature being at 80^{O}C, the specific wear rate is much lower than in the dry contact conditions. It can be said that the presence of the oil in the interface significantly reduces the specific wear rate due to the reduction in the interaction between the asperities and cleaning the rubbing area rather than cooling the interface only.

ISSN(Online) : 2319-8753
ISSN (Print) : 2347-6710

International Journal of Innovative Research in Science, Engineering and Technology

(An ISO 3297: 2007 Certified Organization)

Website: www.ijirset.com

Vol. 6, Issue 2, February 2017

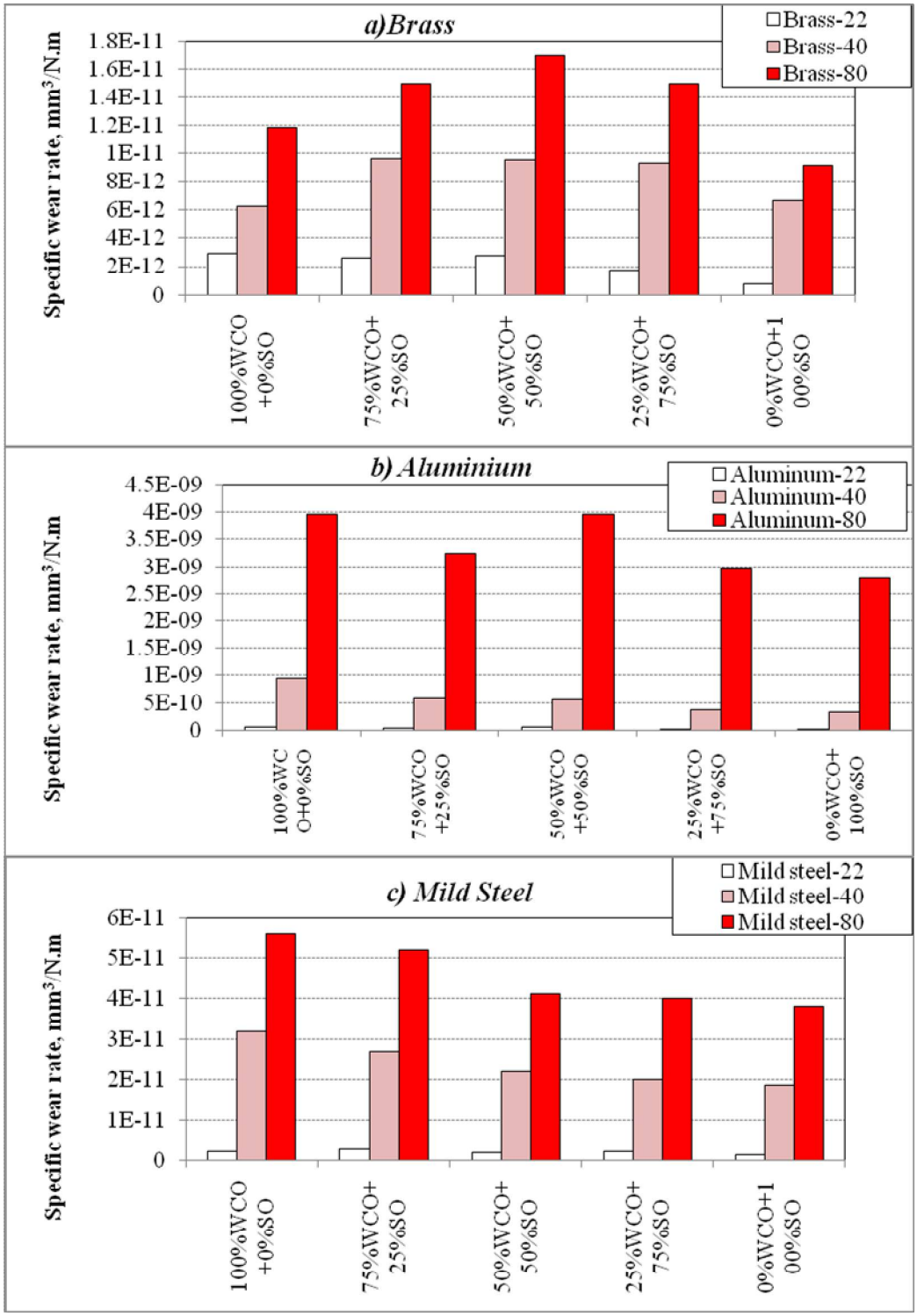

Figure 5.1: Specific wear rate of different materials after 10.8 km sliding distance using different lubricants under different environmental temperatures

ISSN(Online) : 2319-8753
ISSN (Print) : 2347-6710

International Journal of Innovative Research in Science, Engineering and Technology

(An ISO 3297: 2007 Certified Organization)

Website: www.ijirset.com

Vol. 6, Issue 2, February 2017

Figure 5.21 shows that the mild steel and the brass materials seem to be less sensitive to the changes in viscosity of the lubricant due to the changes in the temperature. This could be due to the greater hardness of those materials compared to the aluminium. Although there is low a possibility of separation between the asperities, with the usage of the low viscosity of lubricant, the mild steel and the brass had higher resistance to material removal compared to the aluminium. However, mild steel exhibited slightly higher material removal compared to the brass especially at higher lubricant temperatures, which could be due to the differences in the interaction between the asperities in contact. Since the mild steel has greater strength and hardness, there is high shear in the interface which may lead to an aggressive rubbing process, i.e. high material removal. For the brass, the intermediate properties compared to aluminium and mild steel may mean the contacted asperities have the ability to adapt to each other and the polishing process may have taken place during the rubbing process. Micrographs of the worn surfaces, roughness, and debris micrographs may aid further understanding of this issue.

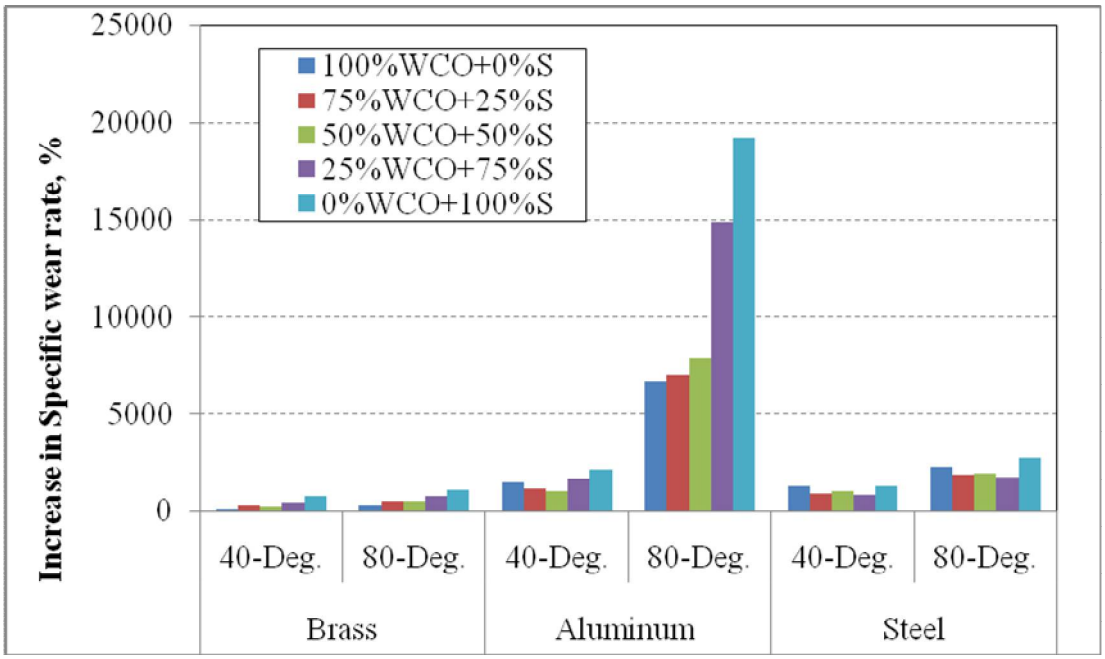

Figure 5.2: Increment percentage in the specific wear rate of different materials after 10.8 km sliding distance using different lubricants under different environmental temperatures compared to the room temperature condition

B. FRICTIONAL BEHAVIOUR

Samples of the friction coefficient against sliding distances for the materials tested at different lubricant temperature with a blend of 50% WCO + 50% SO are introduced in Figure 5.22. At the steady state after about 4 km sliding distance, there is a dramatic increase in the friction coefficient of all the materials when the lubricant temperature increases representing the high interaction between the asperities.

ISSN(Online) : 2319-8753
ISSN (Print) : 2347-6710

International Journal of Innovative Research in Science, Engineering and Technology

(An ISO 3297: 2007 Certified Organization)

Website: www.ijirset.com

Vol. 6, Issue 2, February 2017

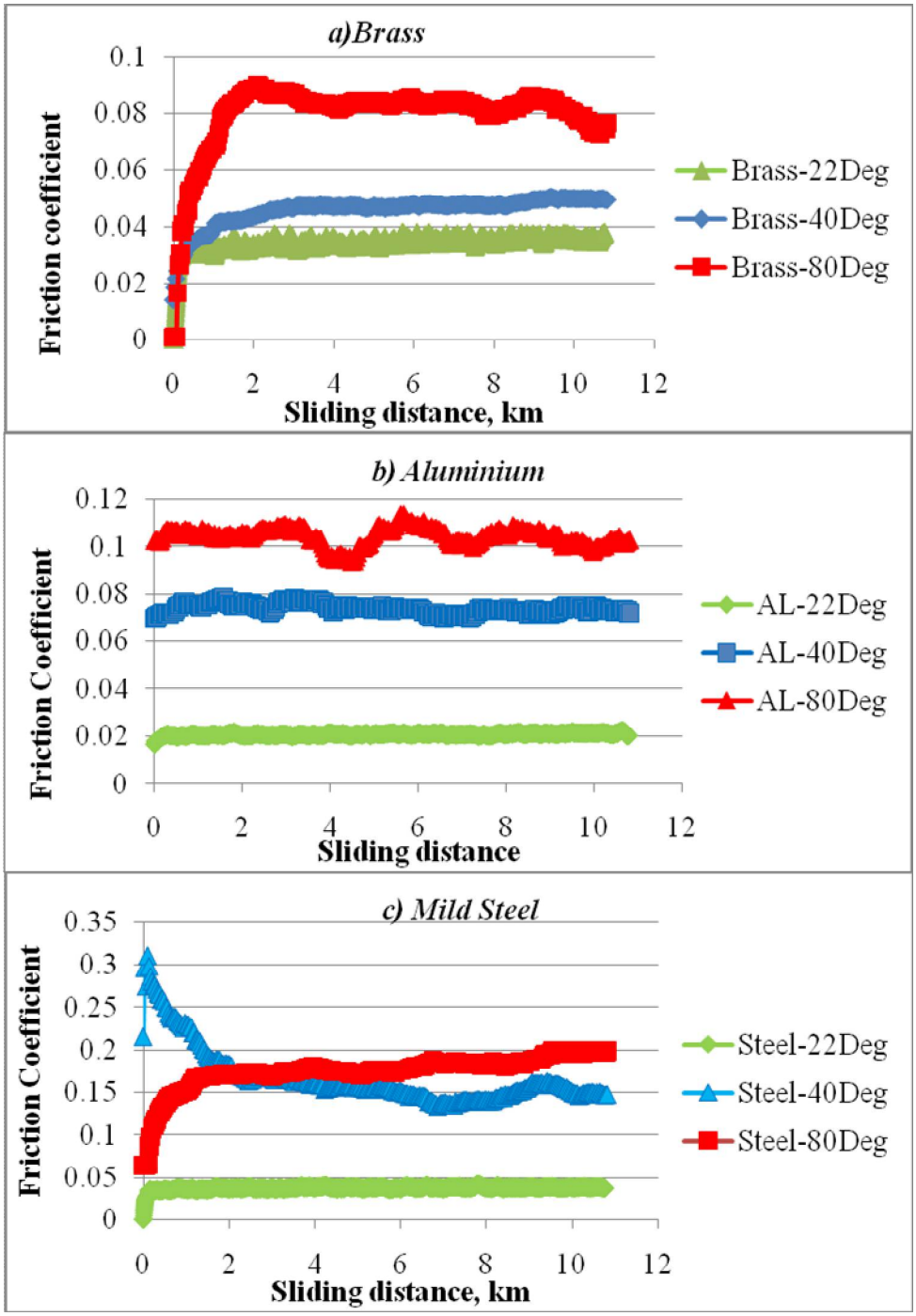

Figure 5.3: Friction coefficient *vs.* sliding distance of different materials tested under 40 N applied load using lubricant (50%WCO + 50%SO) under different temperatures

The mean friction coefficients of brass, aluminium and mild steel under different lubricant conditions and temperatures are presented in Figure 5.23. One can see that the increase in the temperature increased the friction coefficients for all

ISSN(Online) : 2319-8753
ISSN (Print) : 2347-6710

International Journal of Innovative Research in Science, Engineering and Technology

(An ISO 3297: 2007 Certified Organization)

Website: www.ijirset.com

Vol. 6, Issue 2, February 2017

the materials with all the types of blends. The maximum friction coefficient can be seen with high temperature and the usage of the pure WCO. This is mainly due to the fact that the lowest viscosity of all the blends used is the pure WCO at the high temperature. The highest friction coefficient can be seen when the mild steel was rubbed with the presence of the WCO at a temperature of 80°C.

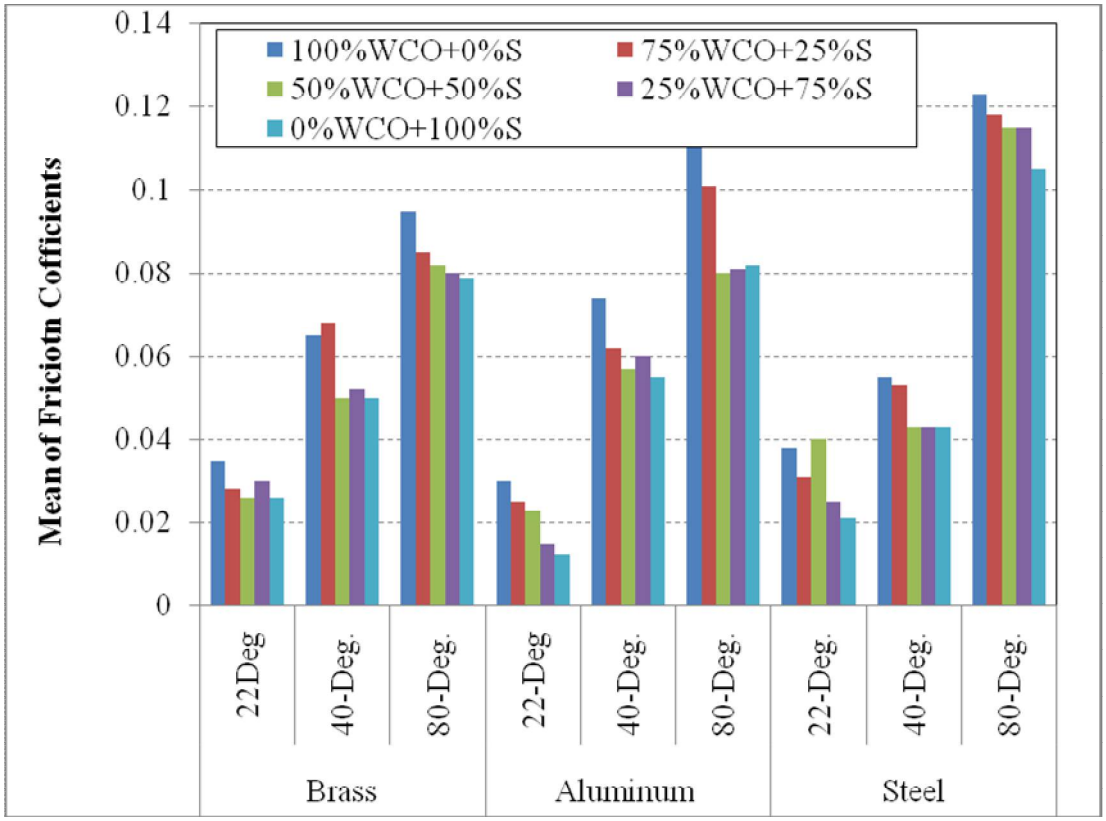

Figure 5.4: Mean values of friction coefficients for all the materials tested under different lubricants and different environmental temperatures

It should be mentioned here that the friction coefficients of aluminium, brass and mild steel were in the ranges of 0.1–0.2, 0.2–0.4 and 0.3–0.35, respectively. Despite the low viscosity of the lubricant at high temperature, there is a comparable reduction in the friction coefficients compared to dry contact conditions. It is known that the presence of the oil in the interface washes the interface and reduces the interaction between the asperities, which in turn reduces the friction coefficient compared to dry conditions. However, the low viscosity of the oil may assist in cleaning the interface but not completely prevent the interaction between the asperities. Therefore, one can say that the reduction in the friction coefficient when the lubricant is introduced is due to the washing the debris and slightly preventing the interaction between the rubbed surfaces (i.e. mixed lubrication region). Similar findings have been reported when sunflower, soybean and castor oils, blended with 4% (w/w) of EVA and 1% (w/w) were tested recently by [26]. The increase in the temperature of (especially) the soybean oil reduced the viscosity, which in turn increased the wear and friction of the steel/steel contact. Velkavrh and Kalin [31] suggested the same regarding the influence of the lubricant viscosity on the friction coefficient of diamond-like carbon coatings and steel.

ISSN(Online) : 2319-8753
ISSN (Print) : 2347-6710

International Journal of Innovative Research in Science, Engineering and Technology

(An ISO 3297: 2007 Certified Organization)

Website: www.ijirset.com

Vol. 6, Issue 2, February 2017

C. SURFACE OBSERVATION

This section covers the roughness of the worn surfaces, micrographs of the worn surfaces and the debris analysis. Samples of the roughness of the metals are given in Figures 5.24 and 5.25 for the worn surfaces of the selected metals under the conditions of 50% WCO and 50% SO as lubricant at elevated temperatures of 40 ^{o}C and 80^{o}C.

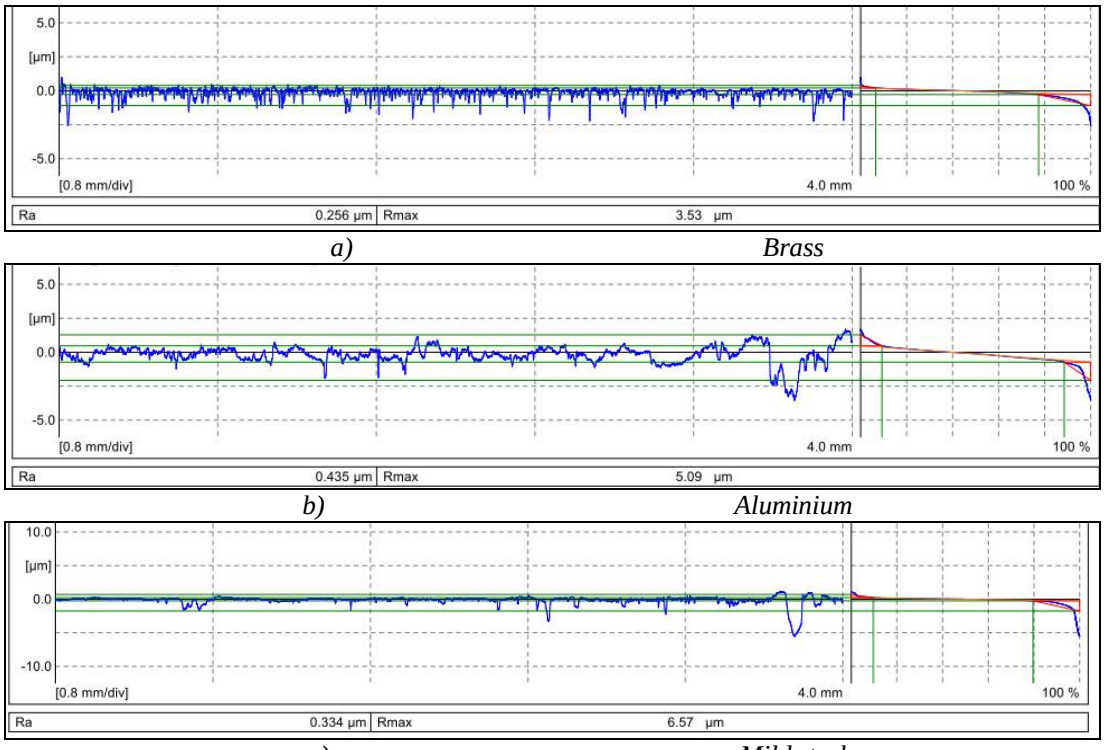

Figure 5.5: Sample of the roughness of the worn surfaces under the condition of 50% waste cooking oil and 50% synthetic oil as a lubricant at elevated temperature of 40^{o}C

ISSN(Online) : 2319-8753
ISSN (Print) : 2347-6710

International Journal of Innovative Research in Science, Engineering and Technology

(An ISO 3297: 2007 Certified Organization)

Website: www.ijirset.com

Vol. 6, Issue 2, February 2017

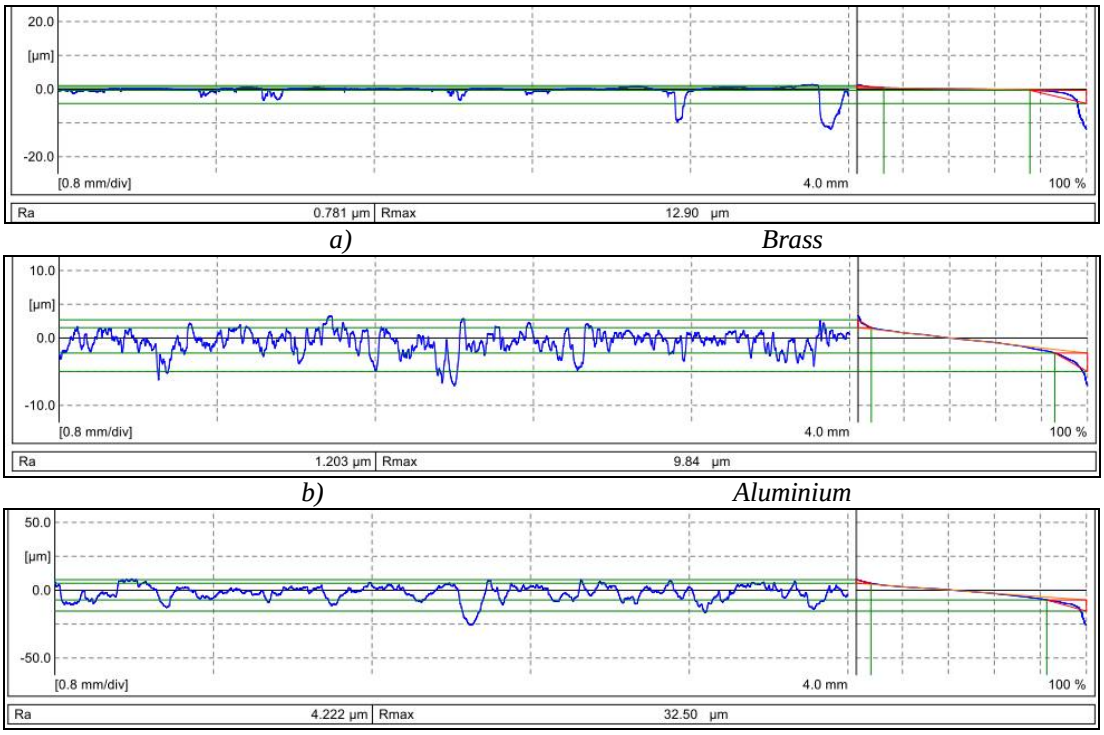

Figure 5.6: Sample of the roughness of the worn surfaces under the condition of 50% waste cooking oil and 50% synthetic oil as a lubricant at elevated temperature of 80^{o}C

A summary of five readings for the same sample of worn surface is presented in Figure 5.26 for all the materials tested under different lubricants and their temperatures. It seems that the increase in the temperature increases the roughness of the surface especially for the mild steel and the aluminium when lubricant at 80^{o}C is used. The increase in the roughness of the metals indicates the severity of the counterface attack on those materials despite the lubricant presence. This is highly pronounced on the mild steel worn surface and aluminium. This may help to understand the significant increase in the specific wear rate of those materials when the lubricant temperature increased (Figure 5.21). Further, the increase in the friction coefficient of the materials with the increase of the lubricant temperature (Figure 5.22) represented resistance in the interface, which can be explained with the increase of the roughness of the worn surfaces. Referring to Figure 4.9, the roughness of the worn surfaces for the steel and aluminium was above 3 µm and about 1 µm, respectively. In other words, the presence of the lubricant at high temperature managed to reduce the interaction between the asperities and somehow achieved less roughness on the worn surface compared to dry contact.

ISSN(Online) : 2319-8753
ISSN (Print) : 2347-6710

International Journal of Innovative Research in Science, Engineering and Technology

(An ISO 3297: 2007 Certified Organization)

Website: www.ijirset.com

Vol. 6, Issue 2, February 2017

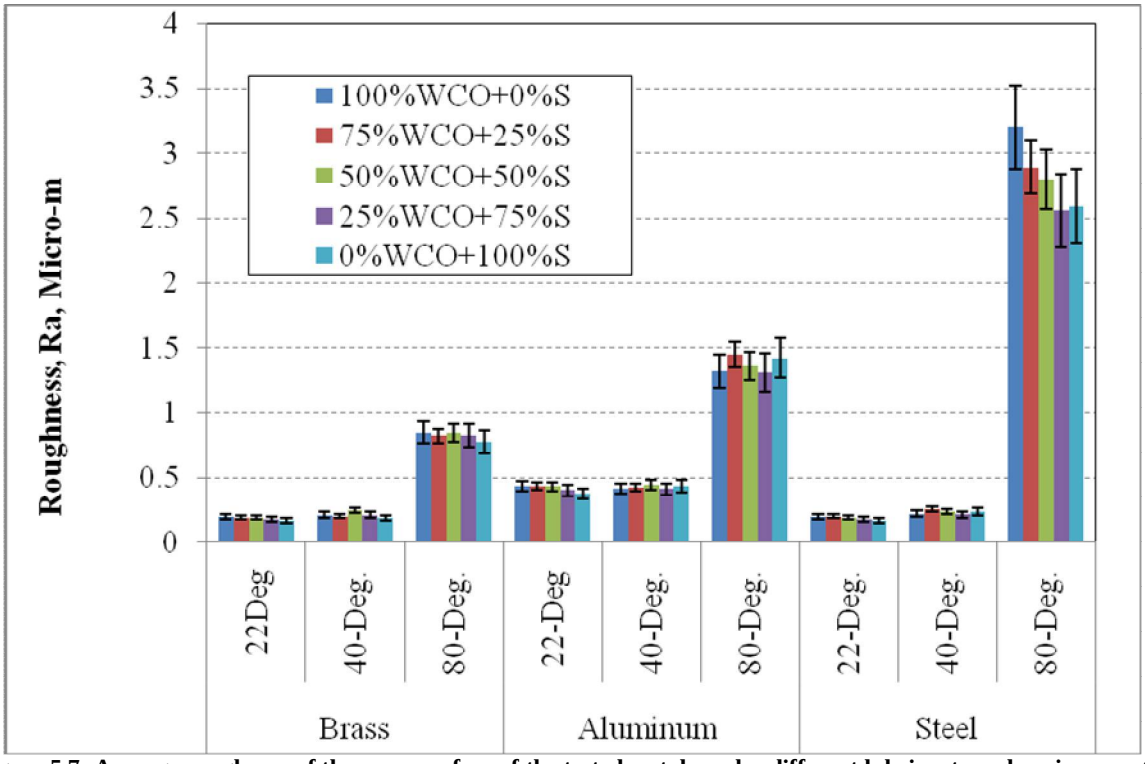

Figure 5.7: Average roughness of the worn surface of the tested metals under different lubricants and environmental temperature.

For the brass materials, there are not many changes in the roughness of the worn material despite the increase in roughness when the temperature was increased to 80^{O}C. Figure 5.27 displays the micrographs of the worn surface of the brass showing a relatively smooth surface compared to the aluminium (Figure 5.28) and the mild steel (Figure 5.29). Figure 5.27 displays the micrographs of brass using lubricant (50% WCO + 50% S) under different environmental temperatures under the applied load of 40 N after 10.8 km sliding distance. In general, the increase in the temperature had an impact on the wear mechanism of the brass, i.e. at high temperature, an increase in the abrasiveness on the surface of the brass can be observed. In comparing Figure 5.27a with Figures 5.27c and d, there is an abrasion nature which can explain the greater roughness of the brass at the higher temperature (Figure 5.26), increase in the friction (Figure 5.23) and significant removal of materials (Figure 5.21). The modification on the worn surface after testing due to the usage of different temperature for the same blends (50% WCO + 50% S) are more pronounced when the aluminium was tested (Figure 5.28). Figures 5.28c and d represent a very rough surface compared to the one tested at low temperature (Figure 5.28a), which indicates the weakness of the surface at these conditions. At the low temperature, the worn surface of the aluminium shows that some of the worn material is still adhered on the surface. In other words, the aggressive abrasion process on the surface of the aluminium could explain the high material removal from the surface, especially at high temperatures (Figure 5.21).

ISSN(Online) : 2319-8753
ISSN (Print) : 2347-6710

International Journal of Innovative Research in Science, Engineering and Technology

(An ISO 3297: 2007 Certified Organization)

Website: www.ijirset.com

Vol. 6, Issue 2, February 2017

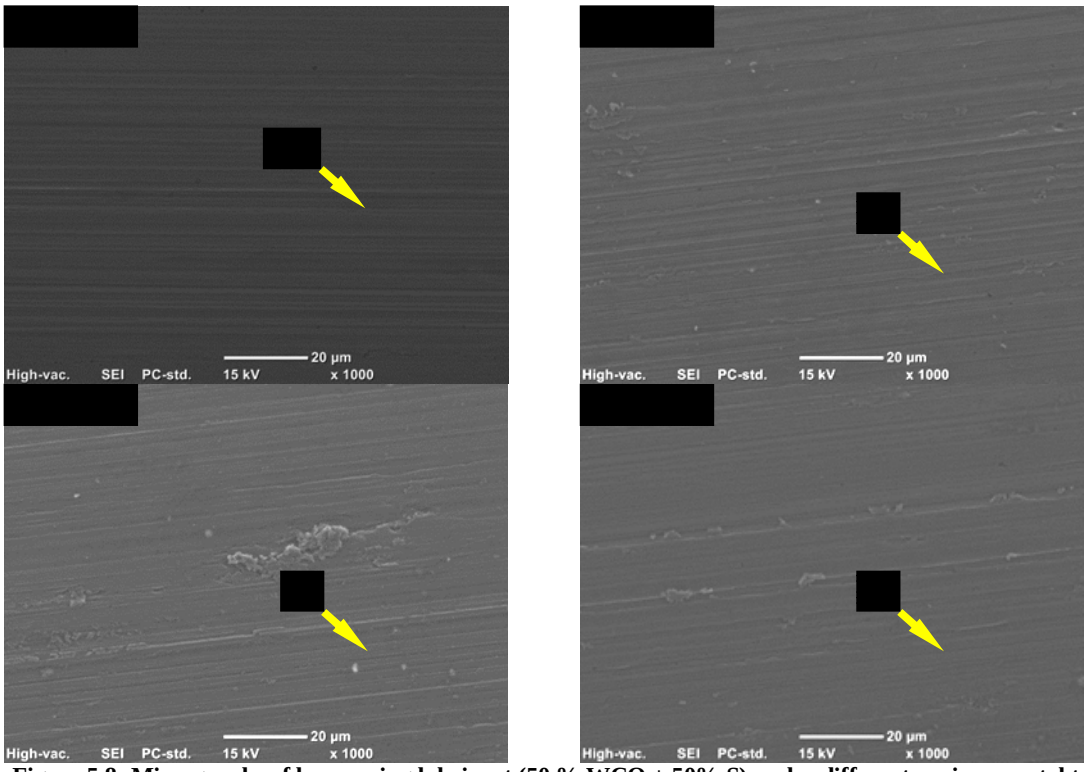

Figure 5.8: Micrographs of brass using lubricant (50 % WCO + 50% S) under different environmental temperatures under the applied load of 40 N after 10.8 km sliding distance showing: abrasive wear mechanism marked as "A"; and adhesive wear marked as "*Ad*"

.

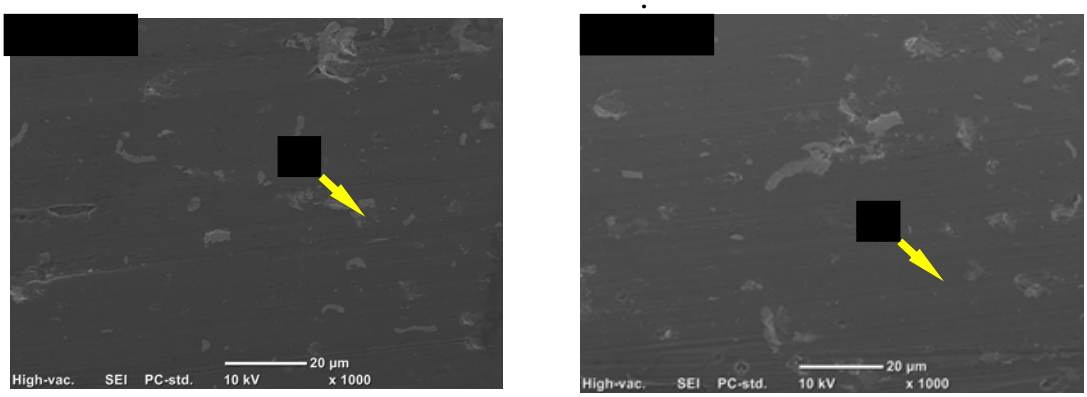

ISSN(Online) : 2319-8753
ISSN (Print) : 2347-6710

International Journal of Innovative Research in Science, Engineering and Technology

(An ISO 3297: 2007 Certified Organization)

Website: www.ijirset.com

Vol. 6, Issue 2, February 2017

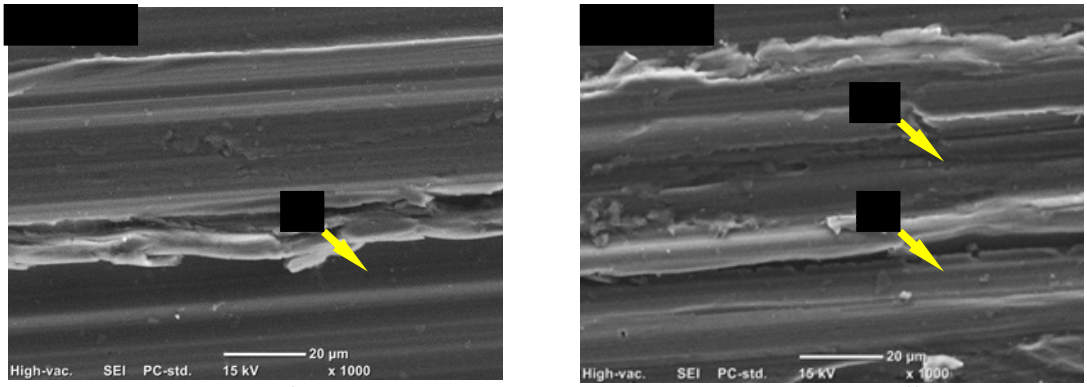

Figure 5.9: Micrographs of aluminium using lubricant (50 % WCO + 50% S) under different environmental temperatures under the applied load of 40 N after 10.8 km sliding distance showing: abrasive wear mechanism "marked as "A"; adhesive wear marked as "*Ad*", and ploughing marked as "*Pl*"

Figure 5.29 displays micrographs of mild steel using lubricant (50 % WCO + 50% S) under different environmental temperatures at the applied load of 40 N after 10.8 km sliding distance. From this figure, one can see that the increase of the temperature from 40^{o}C to 80^{o}C allows the counterface to significantly attack the mild steel surface compared to the low temperature environment. The reason for this is similar to that for the previous example; the increase in the temperature reduced the viscosity, which increased the interaction between the asperities in contact. When the stainless steel counterface rotates against the mild steel sample, an abrasion nature can be seen (Figure 5.26), which leads to a higher friction coefficient (Figure 5.22 c) and higher specific wear rate (Figure 5.20 c) compared to the values at low environmental temperature.

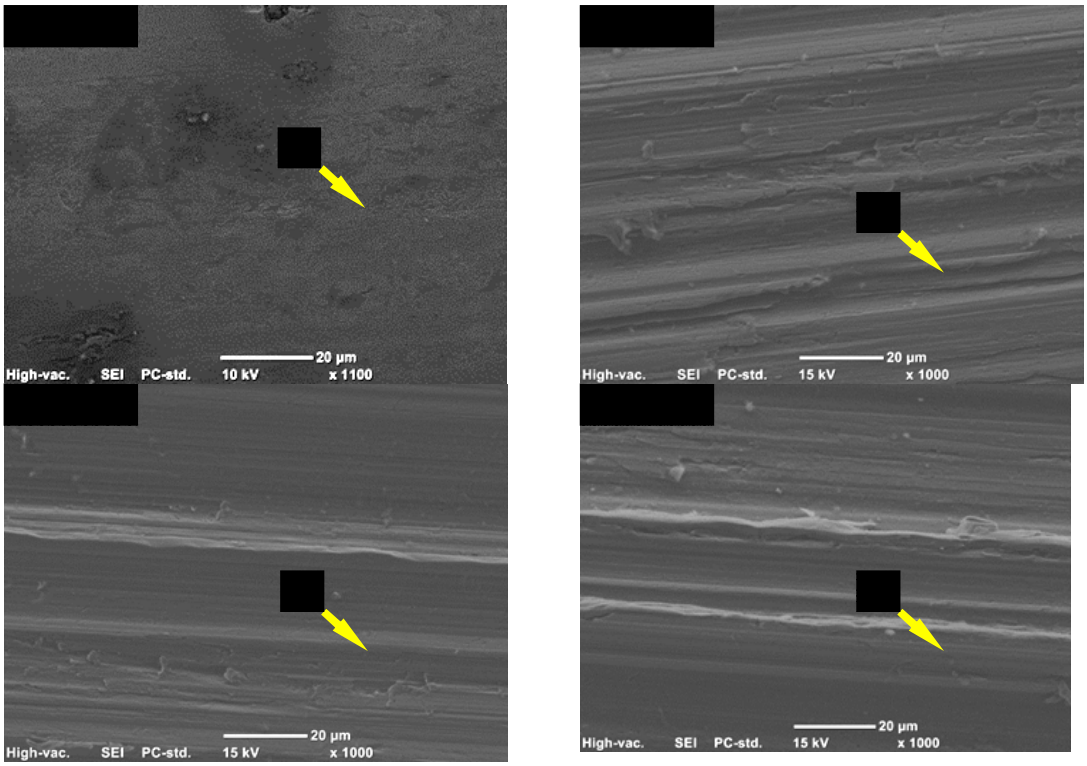

Figure 5.10: Micrographs of mild steel using lubricant (50% WCO + 50% S) under different environmental temperatures under the applied load of 40 N after 10.8 km sliding distance showing: abrasive wear mechanism "marked as "A"; and pitting marked as "*Pt*"

ISSN(Online) : 2319-8753
ISSN (Print) : 2347-6710

International Journal of Innovative Research in Science, Engineering and Technology

(An ISO 3297: 2007 Certified Organization)

Website: www.ijirset.com

Vol. 6, Issue 2, February 2017

The abrasion nature of the worn surface of the mild steel may be due to the presence of the removed debris in the interface, which acted as a third body in the hot lubricant. At the temperature of 80°C, it should be mentioned that the colour of the oil changed during the rubbing process (Figure 5.30). The collected debris was extracted from the oil and then observed using the SEM. Figure 5.31 displays the micrographs of the debris when the mild steel was tested at an elevated temperature. One can see, from Figure 5.29 and Figure 5.31, that there is abrasive two body process occurring during the sliding which is predominant as ploughing.

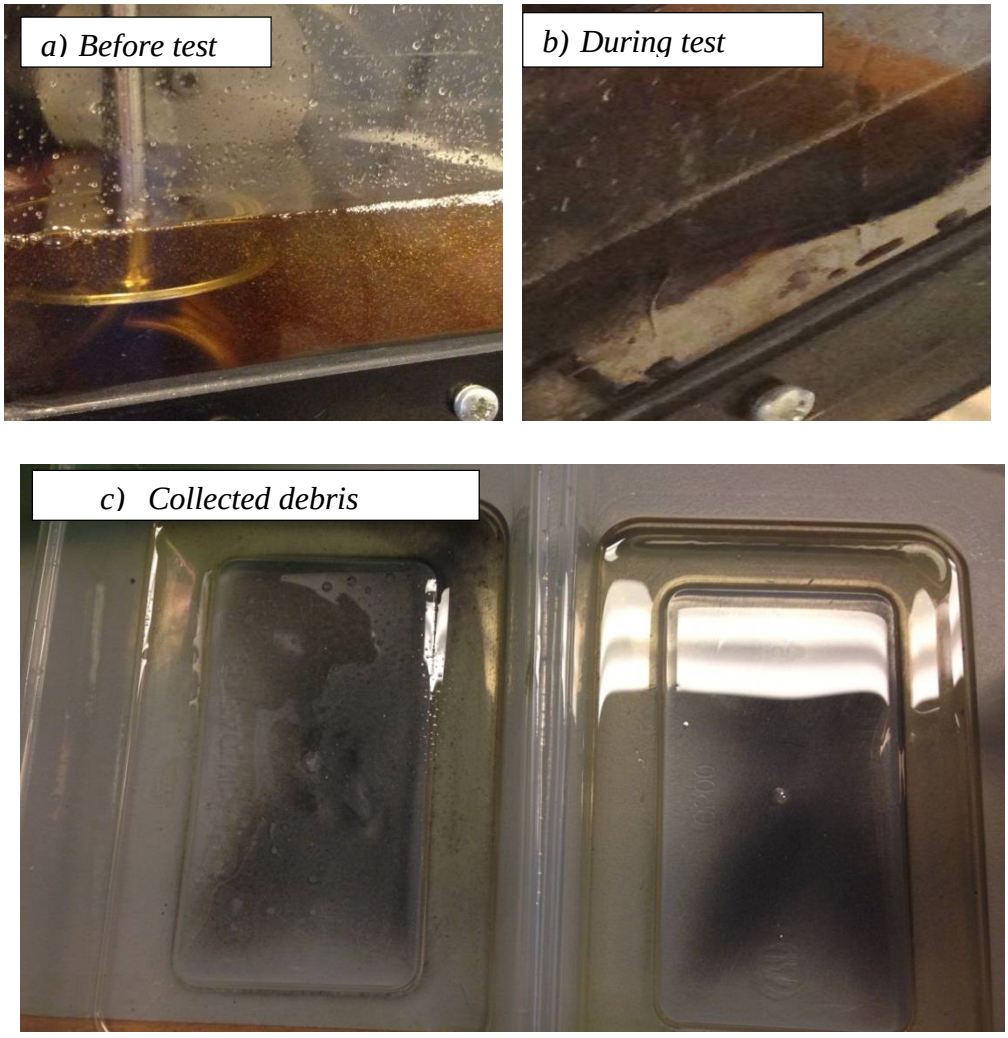

Figure 5.11: Photo showing a sample of the oil when the mild steel was tested using lubricant (50 % WCO + 50% S) at 40 N after 10.8 km sliding distance with environmental temperature of 80°C

The mild steel debris looks like metal fibres, which indicates the large amount of material removed from the mild steel surface. That debris was in the lubricant and rotated and entered the rubbing interface. The naked eyes saw that the colour of all types of lubricant changed dramatically with time. One could see through the side window of the container (Figure 5.30 a, b) the changes in the oil colour. In addition to this, a centrifuge setup was used to extract the debris from the oil as described in Chapter 3, Figure 3.11. This confirms that the debris floated in the lubricant and had the ability to enter the interface. This increased its attachment to both rubbed surfaces leading to high friction and high material

ISSN(Online) : 2319-8753
ISSN (Print) : 2347-6710

International Journal of Innovative Research in Science, Engineering and Technology

(An ISO 3297: 2007 Certified Organization)

Website: www.ijirset.com

Vol. 6, Issue 2, February 2017

removal. It is important to note here that the roughness of the counterface was measured and a pronounced increase in the roughness of the stainless steel counterface was recorded, i.e. ≈ 0.1 µm Ra before testing, and ≈ 1.3 µm Ra after testing. This confirms that the wear mechanism for the mild steel against the stainless steel at elevated lubricant temperature was abrasive wear, which can be categorised as third-body abrasion or two-body abrasion. Under dry contact conditions (Figure 4.12) this abrasion nature was not witnessed. It seems that the presence of the low viscosity oil in the interface of the mild steel/stainless steel contact area prevented the adaption of the two surfaces (no plastic deformation and formation of film) and brought the hard debris (mild steel) to the interface, which attacked both surfaces. For the brass, it was difficult to extract the debris from the oil since it was in very small amounts and difficult to filter. With more than 10 times washing using the acetone and the centrifuge machine to clean the debris from the oil, it was not able to collect the debris and perform the SEM observation.

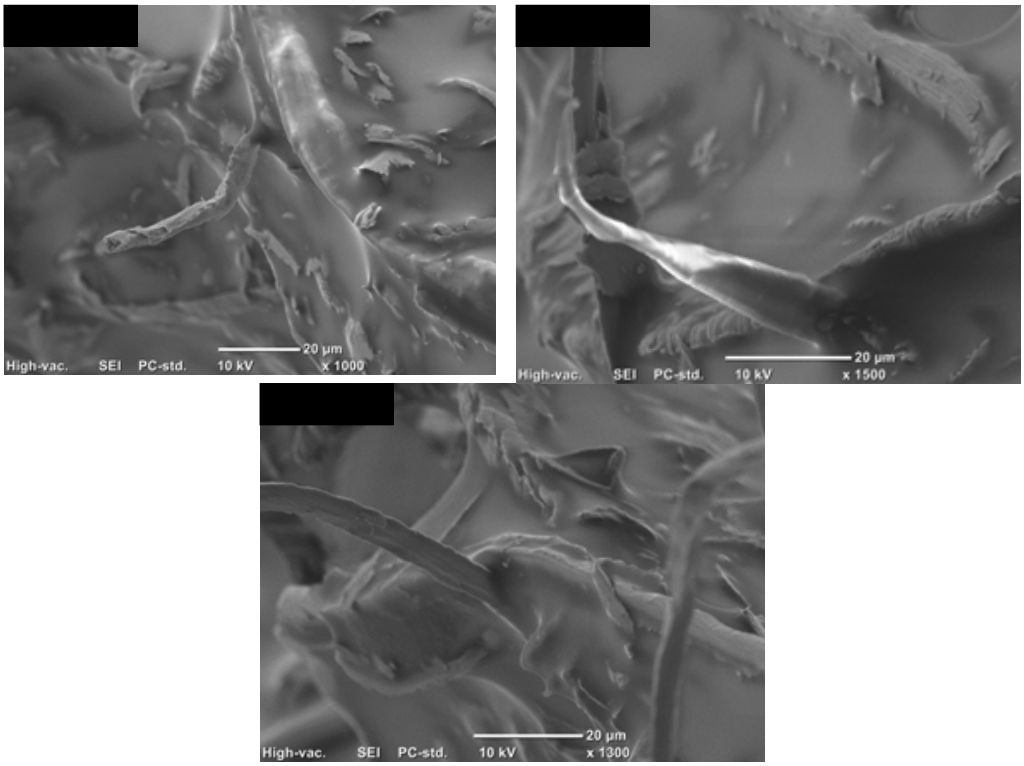

Figure 5.12: Micrographs of mild steel debris after testing using lubricant (50% WCO + 50% S) at 40 N after 10.8 km sliding distance with an environmental temperature of 80°C

Figure 5.32 displays aluminium debris after testing using lubricant (50% WCO + 50% S) at 40 N after 10.8 km sliding distance with an environmental temperature of 80°C. The micrographs of the debris show patches of debris that are different from the one seen in the case of the mild steel (Figure 5.31). It seems that the weakness of the aluminium generated such forms of debris and the presence of such debris in the interface attacked the weak surface (aluminium) more than the stainless steel counterface since it is much harder than the aluminium. The roughness of the counterface increased slightly after testing the aluminium, i.e. from ≈ 0.1 µm Ra before testing to ≈ 0.5 µm Ra after testing.

ISSN(Online) : 2319-8753
ISSN (Print) : 2347-6710

International Journal of Innovative Research in Science, Engineering and Technology

(An ISO 3297: 2007 Certified Organization)

Website: www.ijirset.com

Vol. 6, Issue 2, February 2017

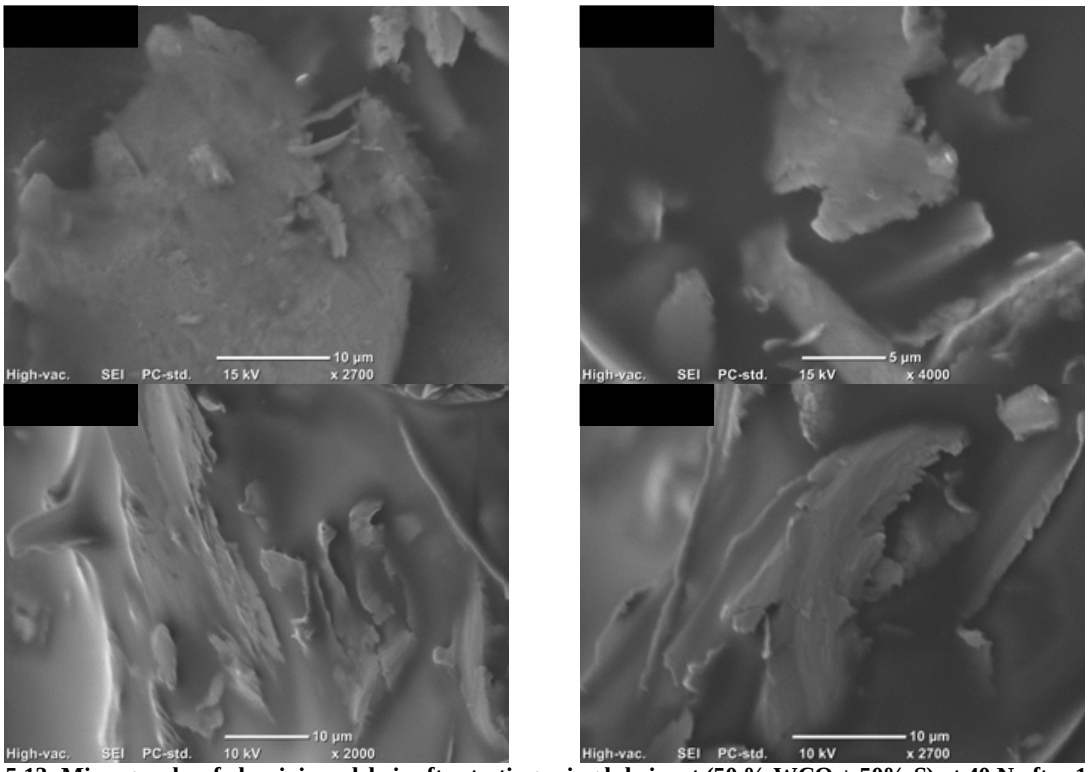

Figure 5.13: Micrographs of aluminium debris after testing using lubricant (50 % WCO + 50% S) at 40 N after 10.8 km sliding distance with environmental temperature of 80^{o}C

The most relevant works have been conducted by [10, 26, 31-35]. All these works are recent and agreed that a reduction in the viscosity for any reason (e.g. type of oil, environmental effect, additives, blend ratio) leads to a high wear rate and friction coefficient for any type of rubbing metals.

VI. CONCLUSIONS

The main findings of the current work can be concluded in the following points:

1. Under dry contact condition, the aluminium materials showed poor tribological results compared to the mild steel and the copper. Also, the materials are very sensitive to the operating parameters since there is significant effect of the applied loads and speed on the wear and the frictional behaviour of those materials.
2. Under lubricant contact condition, dramatical reduction in the wear rate and the friction coefficient were exhibited for all the materials under various operating parameters using all types of blends compared to the dry conditions.
3. The addition of the waste cooling oil in the synthetic deteriorate the viscosity of the oil. However, at low percent of waste cooking oil there is no remarkable modification on the lubricity of the lubricant.
4. The presence of the third body in the lubricant worsened the wear performance of all the materials since the adhesive wear were transferred into third body abrasion which was so noticeable with the aluminium materials.

ISSN(Online) : 2319-8753
ISSN (Print) : 2347-6710

International Journal of Innovative Research in Science, Engineering and Technology

(An ISO 3297: 2007 Certified Organization)

Website: www.ijirset.com

Vol. 6, Issue 2, February 2017

REFERENCES

1. Majdoub, F., et al., *Effect of Temperature on Lubricated Steel/Steel Systems With or Without Fatty Acids Additives Using an Oscillating Dynamic Tribometer.* Tribology Letters, 2014.
2. Ikeda, K., K. Tomohiro, and H. Ito, *Lubricant potentiality of degraded palm oil and effect of free fatty acid addition*. 2014. p. 316-319.
3. Liu, W., J. Zhu, and Y. Liang, *Effect of bridged cyclotriphosphazenes as lubricants on the tribological properties of a steel-on-steel system.* Wear, 2005. **258**(5–6): p. 725-729.
4. Wang, Z., K. Dohda, and Y. Haruyama, *Effects of entraining velocity of lubricant and sliding velocity on friction behavior in stainless steel sheet rolling.* Wear, 2006. **260**(3): p. 249-257.
5. Panagopoulos, C.N., E.P. Georgiou, and K. Simeonidis, *Lubricated wear behavior of leaded α+β brass.* Tribology International, 2012. **50**(0): p. 1-5.
6. Amirat, M., et al., *Influence of the gas environment on the transferred film of the brass (Cu64Zn36)/steel AISI 1045 couple.* Wear, 2009. **267**(1-4): p. 433-440.
7. Erarslan, Y., *Wear performance of in-situ aluminum matrix composite after micro-arc oxidation.* Transactions of Nonferrous Metals Society of China, 2013. **23**(2): p. 347-352.
8. Wang, L., et al., *Identification of a friction model for the bearing channel of hot aluminium extrusion dies by using ball-on-disc tests.* Tribology International, 2012. **50**(0): p. 66-75.
9. Yousif, B.F., *Design of newly fabricated tribological machine for wear and frictional experiments under dry/wet condition.* Materials & Design, 2013. **48**(0): p. 2-13.
10. Shahabuddin, M., et al., *Comparative tribological investigation of bio-lubricant formulated from a non-edible oil source (Jatropha oil).* Industrial Crops and Products, 2013. **47**(0): p. 323-330.
11. Xiao, Y., et al., *The tribological performance of TiN, WC/C and DLC coatings measured by the four-ball test.* Ceramics International, 2014. **40**(5): p. 6919-6925.
12. ASTM G77-98 Standard Test Method for Ranking Resistance of Materials to Sliding Wear Using Block-on-Ring Wear Test, W.C.
13. Rahman, S., et al., *Effect of idling on fuel consumption and emissions of a diesel engine fuelled by Jatropha biodiesel blends.* Journal of Cleaner Production, 2014.
14. Quinchia, L.A., et al., *Low-temperature flow behaviour of vegetable oil-based lubricants.* Industrial Crops and Products, 2012. **37**(1): p. 383-388.
15. Asadauskas, S. and S.Z. Erhan, *Depression of pour points of vegetable oils by blending with diluents used for biodegradable lubricants.* Journal of the American Oil Chemists' Society, 1999. **76**(3): p. 313-316.
16. Bezergianni, S., A. Dimitriadis, and L.P. Chrysikou, *Quality and sustainability comparison of one- vs. two-step catalytic hydroprocessing of waste cooking oil.* Fuel, 2014. **118**(0): p. 300-307.
17. Cao, L., et al., *Ethyl acetoacetate: A potential bio-based diluent for improving the cold flow properties of biodiesel from waste cooking oil.* Applied Energy, 2014. **114**(0): p. 18-21.
18. Ting, C.-C. and C.-C. Chen, *Viscosity and working efficiency analysis of soybean oil based bio-lubricants.* Measurement, 2011. **44**(8): p. 1337-1341.
19. Brockwell, K., W. Dmochowski, and S. Decamillo, *An investigation of the steady-state performance of a pivoted shoe journal bearing with ISO VG 32 and VG 68 oils.* Tribology transactions, 2004. **47**(4): p. 480-488.
20. Stachowiak, G. and A.W. Batchelor, *Engineering tribology*. 2013: Butterworth-Heinemann.
21. *Mixed-fiber diets and cholesterol metabolism in middle-aged men.* Nutr Rev, 1991. **49**(3): p. 80-2.
22. Rudnick, L., *Automotives Gear Lubricants, Synthetics, mineral oils, and bio-based lubricants: chemistry and technology.* 2006, Taylor and Francis, Florida.
23. Rudnick, L.R., *Lubricant additives: chemistry and applications*. 2010: CRC Press.
24. Quinchia, L.A., et al., *Viscosity modification of different vegetable oils with EVA copolymer for lubricant applications.* Industrial Crops and Products, 2010. **32**(3): p. 607-612.
25. Yang, D., et al., *"Green" films from renewable resources: Properties of epoxidized soybean oil plasticized ethyl cellulose films.* Carbohydrate Polymers, 2014. **103**(0): p. 198-206.
26. Quinchia, L.A., et al., *Tribological studies of potential vegetable oil-based lubricants containing environmentally friendly viscosity modifiers.* Tribology International, 2014. **69**(0): p. 110-117.
27. Paredes, X., et al., *High pressure viscosity characterization of four vegetable and mineral hydraulic oils.* Industrial Crops and Products, 2014. **54**(0): p. 281-290.
28. Madankar, C.S., S. Pradhan, and S.N. Naik, *Parametric study of reactive extraction of castor seed (Ricinus communis L.) for methyl ester production and its potential use as bio lubricant.* Industrial Crops and Products, 2013. **43**(0): p. 283-290.
29. Erhan, S.Z., B.K. Sharma, and J.M. Perez, *Oxidation and low temperature stability of vegetable oil-based lubricants.* Industrial Crops and Products, 2006. **24**(3): p. 292-299.
30. Ciantar, C., et al., *The influence of lubricant viscosity on the wear of hermetic compressor components in HFC-134a environments.* Wear, 1999. **236**(1–2): p. 1-8.
31. Velkavrh, I. and M. Kalin, *Comparison of the effects of the lubricant-molecule chain length and the viscosity on the friction and wear of diamond-like-carbon coatings and steel.* Tribology International, 2012. **50**(0): p. 57-65.
32. Imran, A., et al., *Study of Friction and Wear Characteristic of Jatropha Oil Blended Lube Oil.* Procedia Engineering, 2013. **68**(0): p. 178-185.
33. Abdullah, M.A., et al., *Reducing Wear and Friction by Means of Lubricants Mixtures.* Procedia Engineering, 2013. **68**(0): p. 338-344.
34. Louaisil, K., et al., *Analysis of interface temperature, forward slip and lubricant influence on friction and wear in cold rolling.* Wear, 2009. **266**(1–2): p. 119-128.
35. Tang, Z. and S. Li, *A review of recent developments of friction modifiers for liquid lubricants (2007–present).* Current Opinion in Solid State and Materials Science, (0).